MAKERERE UNIVERSITY

MODELLING OF THE BEHAVIOR OF THE HEATED CRUDE OIL IN EAST AFRICAN CRUDE OIL PIPELINE

BY

AKELLO WINNIE ROVINAH

2022/HD08/645U

BSC MEC (MAK)

SIGNATURE.. DATE 18/06/2026..............................

SUPERVISOR

ASSOC. PROF. DR. LUBWAMA MICHEAL

SIGNATURE.. DATE 18/6/2026..............................

SUPERVISOR

ASSOC. PROF. DR. MACKAY OKURE

SIGNATURE.. DATE 24/6/2026..............................

A RESEARCH DISSERTATION SUBMITTED TO THE DIRECTORATE OF RESEARCH AND GRADUATE TRAINING FOR THE AWARD OF THE DEGREE OF MASTER OF SCIENCE IN MECHANICAL ENGINEERING OF MAKERERE UNIVERSITY

KAMPALA, UGANDA

JUNE 2026

DECLARATION

I Akello Winnie Rovinah a student at Makerere University College of Engineering Art Design and Technology pursuing a master's degree in mechanical engineering do declare that this study entitled MODELLING OF THE BEHAVIOR OF THE HEATED CRUDE OIL IN EAST AFRICAN CRUDE OIL PIPELINE is my original work and has not been submitted for any other degree award to any other University before.

Akello Winnie Rovinah

2022/HD08/645U

Signature ……Rvinah……………………

Date……18|06|2026………………

APPROVAL

This is to certify that this dissertation has been submitted for examination under my supervision and approval;

1. ASSOCIATE. PROFFESSOR. DR MICHAEL LUBWAMA

Department of Mechanical Engineering,

College of Engineering Design, Art and Technology,

Makerere University

Signature……………………………………………………………Date…18/6/2026……

2. ASSOCIATE. PROFFESSOR. DR. MACKAY OKURE

Department of Mechanical Engineering,

College of Engineering Design,

Art and Technology,

Makerere University

Signature ……………………………………………………………Date…24/6/2026……

ACKNOWLEDGEMENT

The successful completion of this research dissertation has been a significant journey, one that would not have been possible without the unwavering support, guidance, and encouragement of numerous individuals and institutions. It is with profound gratitude that I acknowledge their contributions.

First and foremost, I extend my deepest and most sincere appreciation to my academic supervisors, Associate Professor Dr. Lubwama Michael and Associate Professor Dr. Mackay Okure. Their invaluable guidance, insightful critiques, and steadfast encouragement throughout this research process have been instrumental. Their expertise and patience in steering this work from conception to completion are deeply appreciated.

My heartfelt gratitude goes to my beloved spouse, Capt. Dr. Kamukama Adams, whose support has been my cornerstone. Thank you for your immense financial and academic support, for painstakingly helping me prepare for presentations, for your diligent proofreading, and for consistently tracking my progress to ensure I stayed on course. Your unwavering belief in me has been my greatest motivation.

I am profoundly thankful to my employer, Mr. Bernard Ongodia, the Principal of the Uganda Petroleum Institute, Kigumba, for granting me the time and flexibility to pursue my studies. His understanding and support were crucial in balancing my professional responsibilities with my academic commitments.

I also wish to express my gratitude to the team at Worley and the East African Crude Oil Pipeline (EACOP) Limited for the indirect insights and the professional context that enriched this study.

To my classmates, I offer my sincere thanks for the constructive peer reviews, the stimulating discussions, and the moral support that kept my spirits high throughout this challenging period.

To my dear children, Daniella Karungi Kamukama, Victoria Nankunda Kamukama, and Grace Namwesiga Kamukama, I owe a special debt of gratitude. Thank you for your incredible patience and for enduring the many moments I spent away from you to focus on this work. You are my inspiration.

Finally, I acknowledge Makerere University, Directorate of Research and Graduate Training, the College of Engineering Art and Design, School of Engineering and Mechanical Department for providing the academic platform and resources that made this study possible.

To all who contributed in different ways, please accept this as a token of my sincerest appreciation.

Akello Winnie Rovinah

ABSTRACT

The East African Crude Oil Pipeline (EACOP) is designed to transport waxy crude oil from Uganda to the port of Tanga, Tanzania. Uganda's crude oil has a uniquely high pour point of 40°C, making active heating necessary for flow assurance. This research developed an integrated numerical model (Finite Element Method (FEM) and Computational Fluid Dynamics (CFD) in ANSYS) to simulate the behavior of heated crude oil in the East African Crude Oil Pipeline (EACOP) under normal and failure scenarios. The specific objectives were to quantify radial heat loss across the pipe cross-section for different crude oil fill levels (full, ¾, ½, ¼ bore) and ambient soil temperatures (18 °C to 35 °C), to simulate temperature, velocity, and viscosity profiles along an 18 m pipeline section for five scenarios (normal operation: 50 °C inlet temperature with 70 °C heat trace , heating failure at 50 °C and 40 °C inlet temperature) and to assess the impact of a 20 mm wax layer on those profiles under heating failure at the same two inlet temperatures. The key findings were firstly, the polyurethane foam (PUF) layer contributed 97.8 % of the total thermal resistance, heat loss varied by 32.8 % across the soil temperature range and fill level had a negligible effect when crude oil was present in the pipe. Secondly, under normal heating, the temperature drop was only 2-3 °C over 18 m and viscosity remained constant; without heating and with a 40 °C inlet, the crude oil cooled below its pour point (36.5 °C) and viscosity increased by 300 %. Thirdly, a 20 mm wax layer caused a 31-47 % velocity increase: however, while offering a minor thermal insulation (10 % reduction in cooling rate). The FEM cross-sectional results were validated against the analytical multi-layer conduction solution with a deviation <0.2 %. The study concluded that EACOP's heated and insulated design is sound, but operational success requires maintaining the inlet temperature above 50 °C, proactive pigging before wax reaches 20 mm, and dynamically adjusting heating power according to soil temperature variations.

Keywords: East African Crude Oil Pipeline, thermal-fluid behavior, numerical modeling, Computational Fluid Dynamics, waxy crude oil, Uganda, flow assurance, wax deposition

TABLE OF CONTENTS

LIST OF FIGURES

LIST OF TABLES

LIST OF ACRONYMS

API	American Petroleum Institute
CFD	Computational Fluid Dynamics
CNOOC	China National Offshore Oil Corporation
EACOP	East African Crude Oil Pipeline
FBE	Fusion Bonded Epoxy
FDM	Finite Difference Method
FEM	Finite Element Method
FID	Final Investment Decision
GPU	Graphics Processing Unit
HDPE	High-Density Polyethylene
MoU	Memorandum of Understanding
NDP	National Development Plan
NSE	Navier-Stokes Equation
PUF	Polyurethane Foam
SDG	Sustainable Development Goal
TPDC	Tanzania Petroleum Development Corporation
UNOC	Uganda National Oil Corporation
UN	United Nation
WAT	Wax Appearance Temperature

CHAPTER ONE: INTRODUCTION

1.1 Background

Uganda's journey into petroleum exploration dates back to the early 20th century, when government geologist E.J. Wayland documented hydrocarbon seepages along the Albertine Graben in the 1920s. These natural oil seeps, particularly near Kibiro on the shores of Lake Albert, marked the first evidence of the country's hydrocarbon potential. The discovery was followed by intermittent exploration activities, including the drilling of Uganda's first deep well, Waki B-1, in 1938. Although exploration slowed during the mid-20th century due to global and political disruptions, renewed efforts in the 1980s through aeromagnetic surveys and seismic studies revitalized interest in Uganda's petroleum prospects. This culminated in significant commercial discoveries in the early 2000s, firmly establishing the Albertine Graben as the nation's most promising petroleum basin and positioning Uganda as an emerging player in Africa's oil industry. (Petroleum Authority of Uganda, 2023).

Uganda has an estimated 6.5 billion barrels of oil in place, of which at least 1.4 billion barrels are recoverable. The signing of the final investment decision (FID) with Total, China National Offshore Oil Corporation (CNOOC), and the government of Tanzania on February 1, 2022, paved way for the construction of the pipeline and the development of the oil fields in order to start oil production by 2025 (Petroleum Authority, 2022). As Uganda progresses towards the exploitation of its oil reserves, there are plans to extract the crude oil and transport it through a 1,443 km East African Crude Oil Pipeline (EACOP) from Uganda to Tanzania, (see Figure 1).

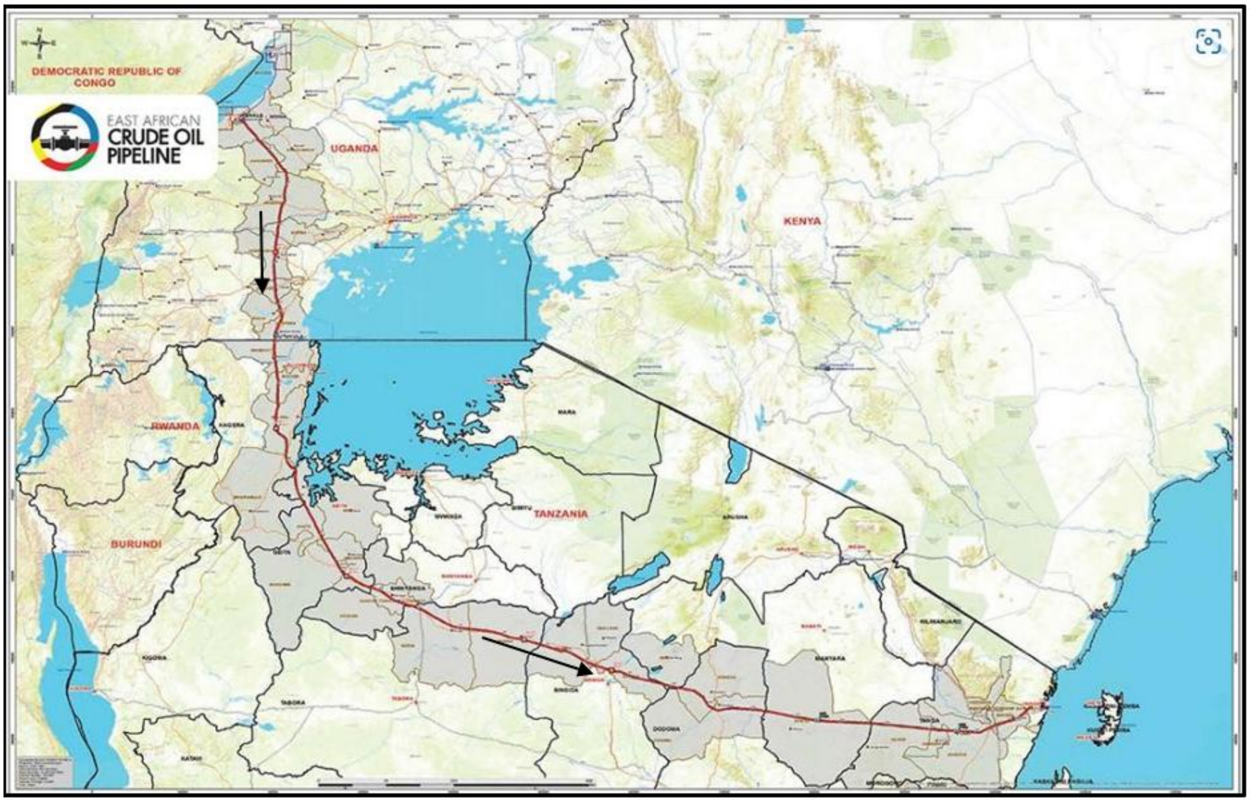

Figure 1: East African Crude Oil Pipeline route (East African Crude Oil Pipeline (EACOP) LTD, 2022)

According to Sonnichsen there was a total of 548 operational oil pipelines in the world as of December 2020 and the number of oil pipelines under construction at that time was 26. In Africa alone there are seven major crude oil pipelines namely; North Africa Pipelines (Algeria, Egypt, Libya, Sudan, Tunisia and Morocco), West Africa Pipelines (Cote d'Ivoire, Gabon, Angola, Democratic Republic of the Congo, Chad, Cameroon and Ghana) Nigeria Pipelines, South Africa pipeline, Mozambique pipeline and Zimbabwe Pipelines and the East Africa Pipelines (Kenya, Uganda, Tanzania and Zambia) (Adeola, et al., 2021).Crude oil pipelines play an important role in the global energy infrastructure, acting as the distribution systems that transports essential resources to the core of the energy industry. These pipelines are specifically engineered to move crude oil from extraction sites to processing plants. Globally pipelines make transportation of oil and gas products safer and more reliable (Green & Taylor, 2015).

However, pipelines are faced with numerous challenges like nature of crude oil, significant investment in both operational costs and capital expenses, maintenance, terrain and balancing energy needs with environmental concern. Due to the nature of crude oil certain properties such as viscosity, density, corrosiveness and wax content can affect the engineering designs of the pipelines. A case in point is the EACOP that will transport Uganda’s crude oil which has a pour point of 40°C, which solidifies at room temperature making it waxy and has an American Petroleum Institute (API) range of 17 to 33, with a pour point of 40°C making it viscous (PAU, 2021). Transporting such waxy and viscous crude oil by pipeline poses challenges such as increased viscosity, reduced flow rate, and pipe constrictions due to wax deposits. For waxy and viscous crude oil as the temperature decreases, the viscosity increases and the inner diameter of the pipe decreases due to formation of waxy deposits inside the pipe, thus requiring more energy to pump it from one section to another (Mohyaldinn, 2019). In some cases, the wax deposits on the inner walls of the pipe can cause flow constrictions which can lead to emergency shut downs and other safety issues. Hence the EACOP will need to be heated continuously in order to prevent solidification of wax leading to reduction in flow rate and worst-case scenario complete blockage of the pipeline. Consequently, leading to safety shut downs and potential environmental hazards in the effect of pipeline rupture (Christian, et al., 2021).

During the design and daily operations of crude oil pipelines, modelling and simulation are carried out to identify critical parameters and important behavioral changes for decision-making, performance optimization, and safety enhancement. For the EACOP pipeline, which is designed to transport waxy crude oil from Uganda, thermal fluid modeling is critical for ensuring safety, planning maintenance, guaranteeing long-term stability, and confirming economic feasibility. Modelling approach is indispensable for solving complex real-world problems that are difficult to address theoretically and prohibitively expensive to investigate through experimentation alone (Liu, 2018). Modelling and simulation is a cost-effective, rapid, and highly informative method that has been widely used in the oil and gas sector to analyze velocity profiles (Madjid, 2021), heat transfer, and a multitude of other phenomena.

The reviewed literature reveals key gaps in existing pipeline thermal models. Existing tools mainly address fully filled flow, neglecting partial fill effects and the wetted circumference's role in heat loss. Most detailed simulations using Finite Element Method (FEM) and Computational Fluid Dynamics (CFD) focus on subsea pipelines, not buried systems like the EACOP. Moreover, there is a lack of models tailored to East African soil conditions and pipeline geometry, underscoring the need for this research.

This research project is conceived with the understanding that the EACOP pipeline has been designed and is being built however, as those specific models and results are not privy to this academic study. Therefore, this research will develop an independent model to understand the behavior of the heated Uganda's crude oil in the EACOP.

1.2 Problem statement

Uganda's crude oil exhibits unique properties where it solidifies at room temperature due to a pour point of 40°C, resulting in a waxy consistency. It has an American Petroleum Institute (API) gravity ranging from 17 to 33, classifying it as a medium to heavy crude with a corresponding density range of approximately 860 to 952 kg/m³. Transporting such waxy and viscous crude oil through the pipelines presents significant challenges which include increased viscosity, reduced flow rates, and potential pipe constrictions caused by wax deposits. As temperatures decrease, the oil's viscosity rises, and waxy deposits form on the pipe walls, leading to a narrower inner diameter. Consequently, more energy is required to pump the oil. In severe cases, these wax deposits can cause complete flow restrictions, necessitating emergency shutdowns and posing serious safety risks.

Failure to understand the variations in temperature, viscosity, and velocity of the crude oil along the heated pipeline due to reduced heating capacity or total failure of heating systems may result in severe operational problems for example pipe blockage, significantly increasing pumping energy requirements and operational costs. Thus, modelling the behavior of the heated crude oil in the EACOP will give an insight in the flow variations without the need for expensive experiments.

1.3 Objectives

1.3.1 Main objective

The main objective of this research was to develop numerical models that mimic flow of the heated crude oil in the EACOP pipeline under normal and failure scenarios.

1.3.2 Specific Objectives

(i) To design and simulate a FEM model of radial heat loss across the cross section of the pipe for different crude oil fill levels (at full, three quarter, half and quarter filled) and ambient temperatures (18°C to 35°C).

(ii) To design and simulate temperature, velocity, and viscosity CFD model along an 18 m pipeline section for five scenarios: normal operation (50°C inlet, 70°C heat trace) and heating failure at two inlet temperatures (50°C and 40°C).

(iii) To assess the impact of a 20 mm wax layer on temperature, velocity, and viscosity profiles along an 18 m pipeline section for heating failure (50°C and 40°C inlet).

1.4 Research Question

(i) How does the rate of heat lost vary across the cross section of the pipe with different crude oil fill levels (at full, three quarter, half and quarter filled) and ambient temperatures?

(ii) How do the axial profiles of temperature, velocity and viscosity develop along the pipeline under varying heating conditions?

(iii) To what extent does wax deposition thickness alter the temperature, velocity and viscosity along the pipeline?

(iv) How can thermal fluid flow behaviors be simulated accurately?

1.5 Scope

The scope of this research was limited to numerical modelling and simulation of heat transfer across the cross section and the thermo-fluid flow behavior along an eighteen meter (18m) distance of the EACOP pipeline on the Ugandan side, limited to five scenarios of normal operating condition failure of the heating system with varying inlet flow temperatures, and wax deposition with varying inlet temperatures.

1.6 Significance of study

Uganda's decision to invest in oil and gas exploitation gives a transformative opportunity for national economic development. There are various challenges associated with the operation of the pipeline that awaits the EACOP in order to realize the profits in this venture.

Modeling and simulation offer a cost-effective and reliable approach to understanding crude oil behavior, optimizing pipeline design, and enhancing operational safety. The risks associated with transportation of Uganda's crude oil justifies the use of modeling and simulation to study the thermal profile of a section of the EACOP pipeline, focusing on fluid flow and heat transfer dynamics. By doing so, it aims to improve flow assurance, reduce energy losses, and support efficient start-up and shutdown procedures. Beyond the technical benefits, the study builds local expertise in computational fluid dynamics, directly aligning with Uganda's National Development Plan IV by strengthening industrialization, supporting infrastructure development, creating employment opportunities, and advancing climate action. In essence, this research is a strategic enabler of NDP IV's vision, linking technical innovation to national development goals. In addition, the research aligns with key United Nations (UN) Sustainable Development Goals (SDG), including SDG 7 (Affordable and Clean Energy), SDG 9 (Industry, Innovation and Infrastructure), and SDG 13 (Climate Action), by promoting efficient and more sustainable pipeline operations.

1.7 Justification

Modelling and simulating the thermal flow behavior of the EACOP is crucial and it ensures design and operations optimization. Proper heat transfer prevents flow assurance and energy efficiency issues especially for the case of Uganda's waxy and viscous crude oil. Efficient heat transfer reduces energy consumption during transportation, while predictive maintenance detects hotspots and prevents failures. In conclusion, thermal fluid modeling also enhances safety, efficiency, and environmental stewardship.

1.8 Conceptual framework

The conceptual framework of this study as seen in Figure 2 models the EACOP as an integrated thermo-fluid system. The core of the framework is the pipeline system. The system's behavior is driven by three sets of Input Parameters: the inherent fluid properties of Uganda's crude oil, the fixed pipeline design and geometry and the operational and boundary conditions.

These inputs govern the internal physical processes of heat transfer and fluid flow within the system. The outputs of these processes are the thermo-fluid flow profile, characterized by the distributions of temperature, velocity, and viscosity. This profile directly determines the critical performance and flow assurance outcomes, ranging from stable, efficient transport under heated conditions to high-risk scenarios like wax deposition and blockage under heating failure. This comprehensive framework guides the entire research process, from model setup in ANSYS to the analysis and interpretation of the results.

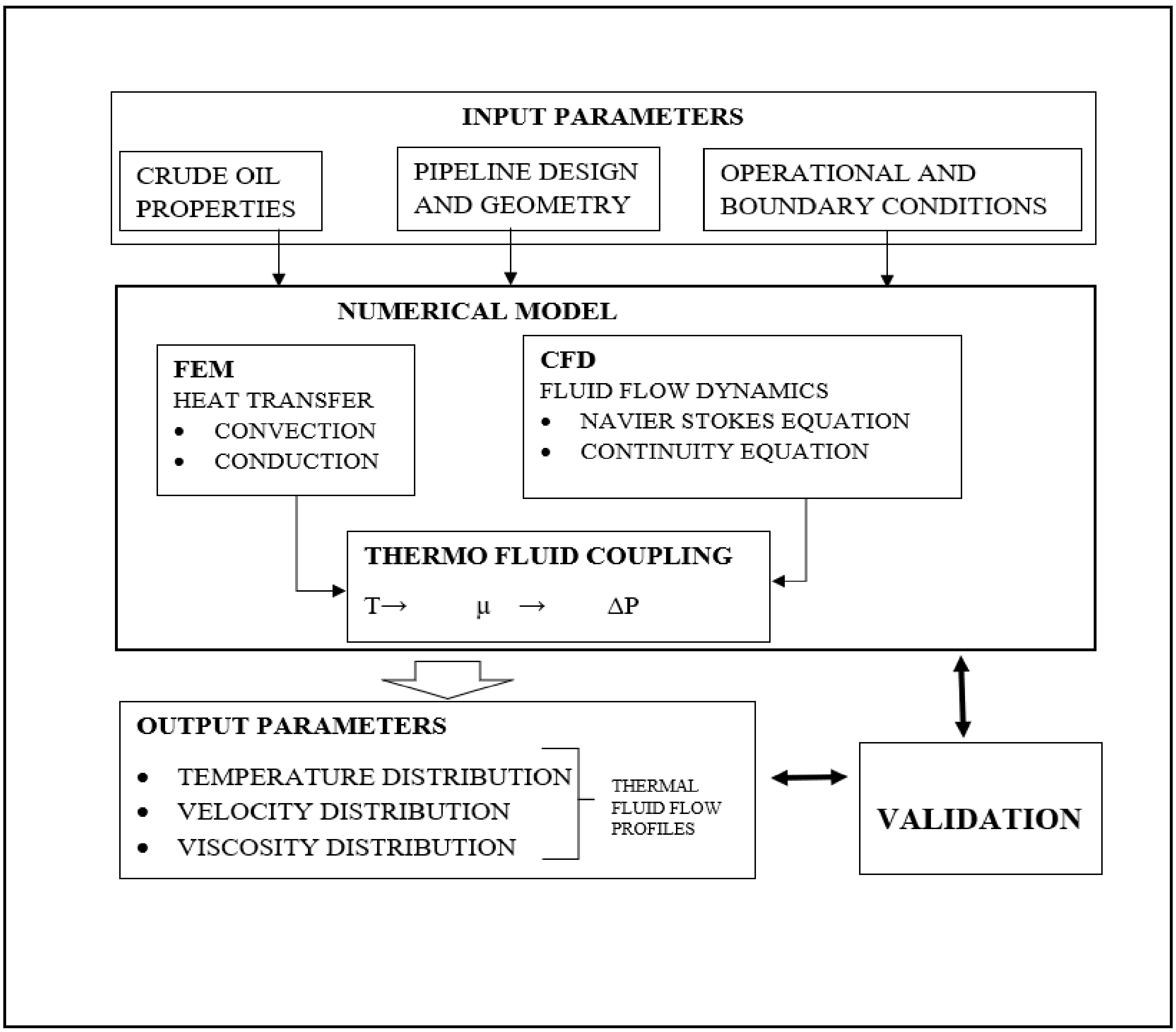

Figure 2: Conceptual framework of the study

CHAPTER TWO: LITERATURE REVIEW

This chapter gives a brief background of the Uganda's crude oil, pipeline decision, EACOP pipeline design, discussion on different modelling methods available, studies on thermal modelling of pipelines, modelling of temperature distributions in pipeline which included classical heat conduction in cylindrical shells, convective boundary layers and partial fill effects, discussion on research done on buried, subsea pipelines, thermal behavior and flow assurance pipeline modelling.

2.1 Uganda's crude oil and pipeline

2.1.1 Uganda's crude oil

In 2006, Uganda's commercial reserves of oil and gas were discovered. The Kingfisher-1 well on the southern end of Lake Albert was the first significant discovery, followed by the Jobi-Rii discovery on the northern end of the lake in 2009 (the largest basin discovery to date) (Edwin, 2022). The oilfields are primarily located in the Albertine Graben, which forms the northernmost part of the western arm of the East African Rift Valley System. This geological scar runs along Uganda's western border with the Democratic Republic of the Congo. The oilfields lie near the shores of Lake Albert (Edwin, 2022). Uganda's crude oil has been characterized as having an API range of 17°C to 33°C. It is considered 'sweet' due to its low Sulphur content. The crude oil is waxy, with an average pour point (the temperature at which it solidifies) of 40°C.This waxy nature can pose challenges during transportation and flow through pipelines. Uganda's crude oil is described as medium to heavy in terms of its viscosity and density (PAU, 2021). Uganda's crude oil reserves are estimated at approximately 6.5 billion barrels, of which 1.4 billion barrels are economically recoverable, with 1.04 billion barrels classified as proven reserves (Ssentamu, 2023)

These characteristics play a crucial role in determining the feasibility of extraction, transportation, and refining processes for Uganda's oil resources.

2.1.2 Uganda's decision to build a pipeline

In accordance with the Memorandum of Understanding (MoU) on the commercialization of Uganda's discovered petroleum resources (Petroleum Authority of Uganda, 2025), feasibility studies on the development of a crude oil export pipeline from Uganda's Albertine Graben to the East African Coast were conducted with the goal of determining the lowest cost route for transporting Uganda's crude oil to international oil markets. The Hoima (Uganda) - Tanga (Tanzania) route was determined to be the most economical and resilient route choice since it was more secure, had fewer construction and logistical restrictions, and already had an operational port, resulting in the lowest potential tariff. This marked the beginning of the East African Crude Oil Pipeline (EACOP) project (PAU, 2023).

2.1.3 Uganda's crude oil pipeline

Uganda's crude oil pipeline has been named the East African Crude Oil Pipeline (EACOP). The EACOP project is being developed, and will be operated by EACOP Ltd, a company composed of Total Energies SE, Uganda National Oil Corporation (UNOC), the Tanzania Petroleum Development Corporation (TPDC) and the China National Offshore Oil Company (CNOOC) (PAU, 2023) and is a significant project that will facilitate the transportation of oil produced from Uganda's Lake Albert oilfields to the port of Tanga in Tanzania. From there, the oil will be sold onward to world markets. The pipeline spans 1,443 kilometers from Kabaale in Hoima district, Uganda, to the Chongoleani Peninsula near Tanga Port in Tanzania. Approximately 80% of the pipeline lies within Tanzanian territory. EACOP is designed to transport two hundred sixteen thousand (216,000) barrels of crude oil per day, with a peak capacity of two hundred forty-six thousand (246,000 barrels per day). The pipeline is buried, allowing people and animals to cross freely once topsoil and vegetation are restored. The EACOP will be continuously heated with heat traces because of the nature of waxy oil Uganda has. There will be heating done by Hydro Electric Power with backup of diesel generators on the Ugandan side while on the Tanzanian side the heating power will be provided by Solar grid power (EACOP LTD, 2022).

2.1.4 Uganda's crude oil pipeline design

The pipeline is made of a 24-inch diameter of steel pipe used in the oil and gas industry of grades of steel of X65 and X60 that meet the American Petroleum Institute (API) 5L standard. The API 5L standard specifies requirements for the manufacture of two product specification levels (PSL1 and PSL2) of seamless and welded steel pipes for use in pipeline transportation systems in the petroleum and natural gas industries. The pipeline is located in an area prone to earthquakes and in such areas, pipelines are designed to withstand seismic activity by incorporating additional safety measures such as thicker walls, stronger materials, and more robust support structures. The steel pipe is surrounded with a Fusion Bonded Epoxy (FBE) coating of 400-600um offering a corrosion resistance. The FBE is engulfed in a Polyurethane foam (PUF)insulation layer of at least 70mm. externally a High-Density Polyethylene (HDPE) casing of 5 to 8mm is used to shield the pipeline from mechanical stress with buoyancy control applied in waterlogged terrains. To enhance monitoring and safety fibre-optic cables are embedded along the pipeline; a 96core main cable supports communication and data transmission while specialized strain-detection fibres are installed in geologically sensitive areas to detect stress and deformation (TotalEnergies, 2021). Additional fibre-optic systems provide real-time surveillance of temperature, vibration, and potential leaks. The trench design, with a burial depth of 1.25 m and a width of approximately 4.5 m, balances protection against external interference with accessibility for maintenance. Supporting systems include high-voltage power cables and a Low-Loss Heat Tracing (LLHT) system, both of which sustain the monitoring infrastructure and ensure crude oil remains within optimal flow conditions (East African Crude Oil Pipeline, 2022). Figure 3 and Figure 4 shows the proposed EACOP. The EACOP employs a network of long-line heat tracing (LLHT) cables running the full 1,443 km, with distributed power supply units placed at regular intervals (every ~30 km) to maintain voltage and ensure uniform heat generation. A centralised SCADA system monitors real-time temperature data and automatically adjusts power to keep the crude oil above its pour point (40 °C). Redundant heating stations at key locations provide additional thermal input when flow rates drop or heat loss increases.

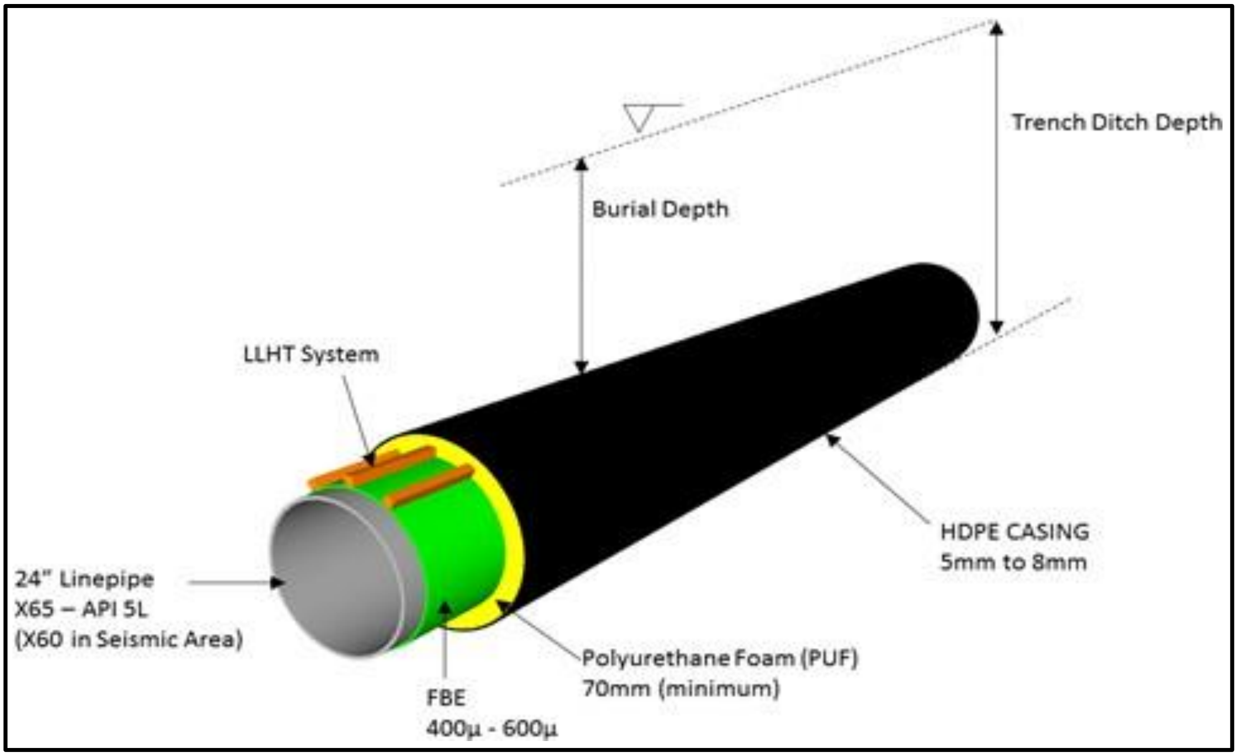

Figure 3: Proposed pipeline EACOP design (East African Crude Oil Pipeline, 2022)

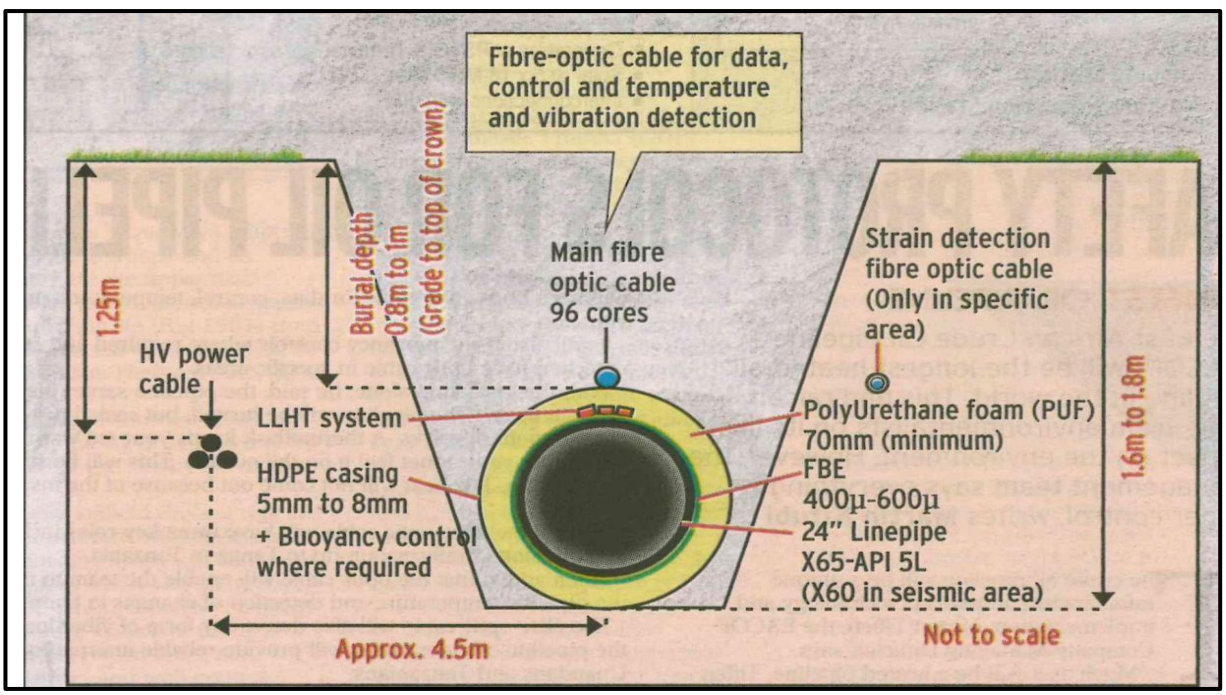

Figure 4: Pictorial representation of pipeline makeup and positioning in the ground (The New Vision, 2022)

2.2 Modelling in pipelines

Fluid modeling refers to the process of mathematically representing the behavior of fluids (liquids and gases) using mathematical equations and computational techniques. It allows researchers to simulate and predict fluid flow, heat transfer, and other related phenomena. By understanding fluid behavior, one can optimize designs, improve operational efficiency, and address real-world challenges.

Fluid modeling plays a crucial role in various Engineering Design and Operations: scientist use fluid modeling to design efficient systems such as pipelines, pumps, and heat exchangers. It also helps to optimize fluid flow patterns, minimize pressure losses, and to enhance performance (MakahlehFiras & Nassar, 2023). Three different methods of fluid modelling are used and these are discussed below with their applications and challenges:

The Finite Difference Method discretizes the Navier-Stokes equations (NSE) on a set of points representing physical variables such as pressure and velocity within the fluid domain. The advantage of FDM is that it’s simple to implement and understand, suitable for structured grids and widely used in introductory CFD courses. FDM has challenges like requiring uniform grid spacing, accuracy depends on grid resolution and limited applicability for complex geometries. FDM is usually used in basic flow simulations and educational purposes (Pei-bai, 1993).

Finite Element Method divides the fluid domain into finite elements, allowing for irregular and unstructured grids. It solves partial differential equations by minimizing energy functional. FEM is versatile for complex geometries, can handles irregular meshes and can model fluid-structure interactions. However, it requires more computational resources, accuracy depends on mesh quality and there are challenging for transient problems. FEM is used in Structural analysis coupled with fluid flow, heat transfer simulations and multiphysics problems (Moukalled, 2016).

Finite Volume Method discretizes the domain into control volumes (cells) and conservatively solves the NSE by balancing fluxes across cell faces. This method conserves mass, momentum, and energy, works well with unstructured grids and is robust for complex geometries. However, it requires careful treatment of boundary conditions, has limited accuracy near discontinuities and may be computationally expensive. It’s used in Turbo machinery design, environmental modeling (Moukalled, 2016).

Computational Fluid Dynamics, is a simulation technique used to analyze and predict the behavior of fluids, such as liquids and gases. It involves solving mathematical equations using computers to model and understand fluid flow, heat transfer, etc. Fluid flow properties (velocity, pressure, viscosity, density, and temperature) are calculated based on defined operating conditions. The governing equations (often based on the Navier-Stokes equations) are solved mathematically (Moukalled, 2016). Thermo-fluid analysis uses conservation laws to govern mass, momentum, and energy, ensuring these remain constant in a closed system. CFD simulations save time and costs, aid in design optimization, and visualize flow patterns, but face challenges like predicting turbulence and requiring accurate data for modeling.

2.3 Studies on thermal modelling of pipelines

For buried pipelines specifically, researchers have established that soil thermal conductivity and burial depth significantly affect heat loss. The concentric-shell method, which reduces the 3D ground problem to a 1D radial conduction model at each axial node, is widely used in industry and academic models (Modisette, 2016; Lanzafame et al., 2017). For partially filled pipes, the inner boundary condition becomes spatially non-uniform: wetted segments have high convective coefficients, while unwetted segments exposed to stagnant air have low convective coefficients. Parallel resistance network models have been developed to account for this effect (Shoushtari et al., 2011; Amran et al., 2024). The practical implication is that equivalent inner-boundary resistance increases as the wetted fraction decreases, reducing radial heat loss for the same bulk fluid temperature.

Despite this established knowledge, three critical gaps persist for the EACOP configuration: No study has quantified the relative contribution of each insulation layer (FBE, steel, PUF, HDPE) to total thermal resistance for a pipeline that is both buried and actively heated. Existing studies focus on either unheated pipelines (where heat loss is purely passive) or subsea pipelines (where boundary conditions differ significantly). The interaction between active heating (heat trace at 70°C) and the multi-layer insulation system has not been analytically validated for EACOP-specific layer thicknesses and material properties. While it is well-known that ambient temperature affects heat loss, the quantitative relationship has not been established for East African soil conditions. Soil temperature in Uganda varies seasonally from approximately 18°C to 35°C (Banage, 1967), yet existing models typically assume constant ambient conditions. The magnitude of heat loss variation across this range remains unquantified. Previous partial-fill studies assume unheated pipes or passive heat transfer. For a heated pipeline, where the heat trace supplies constant power regardless of fill level, the effect of wetted circumference on net heat loss has not been studied. It is unknown whether a partially filled heated pipe loses more or less heat than a filled pipe under the same heating power.

The governing equations for fluid flow and heat transfer in pipes (continuity, Navier-Stokes, and energy equations) are well-established and widely implemented in CFD software. For waxy crude oils, temperature-dependent viscosity is recognized as the single most important parameter for accurate flow prediction (Guillaume et al., 2005; Beloglazov et al., 2021). Research has established that waxy crude oils exhibit strongly non-Newtonian behavior below their wax appearance temperature (WAT). However, above the pour point, the fluid can be reasonably approximated as Newtonian (Guillaume et al., 2005). This is a critical assumption for modelling heated pipelines where temperature is maintained above the pour point. The cooling rate of crude oil along a pipeline follows Newton's law of cooling. This relationship shows that cooling is proportional to the temperature difference between the oil and the surrounding soil, and inversely proportional to flow rate and heat capacity (Wei et al., 2018). Studies on pipeline shutdown and restart (Wei et al., 2018) have demonstrated that cooling rates during flow interruptions can lead to gelation if the crude oil falls below its pour point. The critical importance of maintaining temperature above the pour point is well-recognized in the industry. Recent research has also established quantitative relationships between dimensionless groups. Zhapbasbayev et al. (2024) demonstrated that the Nusselt number increases with Reynolds number and decreases with Bingham number along the pipe length, providing a basis for validating heat transfer coefficients. Furthermore, the inadequacy of one-dimensional modelling for non-isothermal waxy crude flows has been demonstrated. A 2025 study on non-isothermal laminar oil flow in an axisymmetric pipe showed that traditional 1D modelling, which averages temperature and velocity across the pipeline cross-section, cannot fully capture the transition from Newtonian to non-Newtonian behavior caused by temperature drop.

Most research focuses on either steady-state heated operation (where temperature is constant) or complete shutdown (where flow stops). The intermediate scenario of heating system failure with continued flow has not been systematically studied. In this scenario, the crude oil continues to move while cooling, creating a dynamic thermal profile that differs from both steady-state and shutdown conditions. While the Newtonian cooling equation is well-known, the actual cooling rates for a buried, heated pipeline under failure conditions have not been quantified. Specifically, how many degrees per meter does the crude oil lose when heating fails? How long (or how far) before it reaches the pour point? These are critical questions for emergency response planning. Most rheological models are based on crude oils from other regions (North Sea, Gulf of Mexico, China's Qinghai oilfield). Uganda's crude has a uniquely high pour point (40°C) and API range (17-33) (PAU, 2021). The temperature-viscosity relationship for this specific crude has not been published or calibrated in a pipeline CFD context. While velocity is governed by the continuity equation and viscosity is temperature-dependent, the interaction between these variables under heating failure has not been analyzed.

Wax deposition is recognized as a coupled heat and mass transfer problem. Cooling at the pipe wall leads to supersaturation of paraffinic components, diffusion to the wall, nucleation, and deposit growth. Deposit growth then changes thermal resistance and shear conditions, creating a feedback loop that can accelerate deposition (Zhenyu et al., 2011; Giancarlo Giacchetta, 2019). Recent studies have quantified the thermal effect of wax layers. Xie et al. (2022) developed a 3D heat transfer model of a buried crude oil pipeline incorporating a wax layer, finding that even a 4 mm wax layer causes an average soil temperature deviation of 1.42 K. Their work also established that the Effective Medium Theory (EMT) model is most accurate for predicting wax layer thermal conductivity. The hydraulic consequences of wax deposition have been studied through pressure drop measurements. Research has shown that even thin wax layers increase frictional losses due to increased wall roughness and reduced effective flow area (Hoffmann & Amundsen, 2010). Zhapbasbayev et al. (2024) established relationships between Nusselt number, Reynolds number, and Bingham number for viscoplastic waxy oil flows, demonstrating that heat transfer efficiency deteriorates as wax forms and yield stress increases. This creates a feedback loop: cooling promotes wax formation, which reduces heat transfer, which promotes further cooling.

Existing studies focus on the rate of wax deposition under given conditions. They do not answer the operational question: For a given wax layer thickness, what is the impact on flow temperature, velocity and viscosity along the pipeline. This distinction is important because an operator may discover an existing wax layer of unknown age and needs to know the immediate consequences. Most wax deposition models assume continued heating or constant inlet temperature (Xie et al., 2022). The scenario where wax is already present and heating subsequently fails, representing a compounding of two failures has not been studied. The literature has not quantified the relative magnitude of these two opposing effects of wax acting as an insulator or constrictor. The answer determines operational strategy: if thermal benefits dominate, leaving wax in place might be acceptable; if hydraulic penalties dominate, immediate removal is critical.

2.4 Modelling of temperature distribution in a pipeline

Heat transfer between transported crude and the surrounding environment is a central problem in pipeline engineering because thermal losses affect oil viscosity, flow-assurance of buried pipelines. Analytical and numerical methods that quantify radial heat transfer across the pipe cross section provide the engineering basis for operational decisions (insulation, heating, flow rate control) and for coupled thermo-hydraulic models used in pipeline design and operation. The present review summarizes classical heat-conduction theory for cylindrical systems, prior studies of partial-fill and annular convection effects, pipeline thermal modeling approaches used for buried and subsea pipelines, and the link between thermal behavior and wax deposition/flow assurance.

2.4.1 Classical heat conduction in cylindrical shells

The analytical foundation for radial heat transfer in pipes is Fourier’s law applied to cylindrical coordinates. For steady-state radial conduction through a homogeneous cylindrical shell the well-known expression for heat rate per unit length is defined by equation 1.

$$Q = \frac{2\pi(T_i - T_o)}{\ln\left(\frac{r_o}{r_i}\right)} \qquad \text{Equation 1}$$

And the corresponding outer-surface flux is defined by equation 2.

$$q'' = \frac{Q}{2\pi r_o L} \qquad \text{Equation 2}$$

these expressions form the backbone of many first-principles pipeline thermal models and are widely presented in heat-transfer texts and applied studies of pipe thermal performance. The cylindrical conduction solution is commonly combined with convective boundary resistances on the fluid wall and soil wall sides to produce lumped resistance models that are straightforward to evaluate analytically and suitable for sensitivity analyses (Yunus, 2016).

2.4.2 Convective boundary layers and partial-fill effects

When a pipe is partially filled by liquid, the inner boundary condition becomes spatially non-uniform: segments of the inner circumference are in contact with a moving fluid (high convective coefficient) while the unwetted segments are exposed to a stagnant gas (low convective coefficient) or vapour. Shoushtari et al. (2011) modelled such cases by representing the inner boundary as a set of convective arcs or by using equivalent parallel thermal conductances (oil-wetted fraction and air-wetted fraction).

Natural convection in annular gaps is particularly difficult to predict because it depends strongly on geometry, orientation and the Prandtl number; several experimental and numerical studies examine convection in eccentric or partially filled annuli to quantify local heat transfer coefficients and onset of natural convection cells (Amran, Sultan, & Tso, 2024). For pipeline applications, the practical effect is an increase in the equivalent inner-boundary resistance as the wetted fraction decreases, and thus a reduction in radial heat loss for the same bulk fluid temperature (Shoushtari, et al, 2011).

2.4.3 Pipeline thermal models buried and subsea contexts

Applied pipeline thermal modelling typically couples inner convective resistance, pipe wall conduction, and the surrounding ground/sea conduction. Industry and academic models commonly discretize the ground into concentric cylindrical shells or use finite-element/finite-difference approaches to capture transient heat diffusion into the soil or seabed. For buried pipelines this concentric-shell method reduces the 3D ground problem to a 1D radial conduction model at each axial node. Subsea pipelines add complexity from seawater convection, sediment layers, and possible multiphase flow; several studies have compared coupled numerical strategies (e.g. Conjugate heat transfer or FEM for pipe and surrounding medium) and have demonstrated that simpler conductive models can be acceptable when parameterized carefully, but that transient effects and layer heterogeneity (e.g., soft sediments, rock) may require more advanced solutions (Lanzafame, et al, 2017). Present numerical approaches for submarine pipeline heat exchange, comparing conductive FEM solutions with more detailed conjugate models and highlighting the importance of accurate material properties and boundary conditions (Wang, et al 2019) (Modisette, 2016).

2.4.5 Thermal behavior and flow-assurance (wax deposition)

Heat loss has direct operational consequences through its effect on crude viscosity and on the onset of wax crystallization. A substantial body of work models wax deposition as a coupled heat and mass transfer problem like cooling at the pipe wall leads to super saturation and diffusion of heavier paraffinic components, nucleation and deposition; deposit growth then changes thermal resistance and shear conditions, producing a feedback loop. Both empirical sensitivity studies and first-principles models show that small changes in wall temperature or convective heat transfer can significantly affect deposit rate and thickness (Zhenyu, et al, 2011). This demonstrates why accurate estimation of pipe heat loss (including partial-fill cases) is relevant not only to energy budgeting but to long-term operability (Giancarlo, 2019).

CHAPTER THREE: METHODOLOGY

This chapter outlines the methodological framework employed to model and simulate the thermal flow behavior of crude oil along the EACOP. The analysis aims to provide a robust understanding of the temperature-dependent dynamics of crude oil as it moves through the pipeline system under varying operational conditions. The methodology integrates principles of fluid dynamics, heat transfer, and numerical simulation to capture the complex interactions governing thermal behavior.

A combination of analytical modeling and computational techniques was selected to analyze heat loss, velocity variations and viscosity variation along the pipeline length. The main challenge was to capture the temperature-dependent dynamics, especially the drastic increase in viscosity as the oil cools. To address this, a dual numerical approach was used. First, a steady-state Finite Element Method (FEM) model analyzed radial heat transfer across the pipeline's cross-section. Second, a transient Computational Fluid Dynamics (CFD) model simulated axial flow along a section of the pipeline in five cases (for objective 2 (thermo-fluid behavior without wax), three cases were considered: Case 1 (normal operation: 50°C inlet with active heating at 70°C), Case 2 (heating failure only: 50°C inlet with no heating), and Case 3 (low inlet temperature with heating failure: 40°C inlet with no heating), for objective 3 (effect of wax deposition), two additional cases were simulated: Case 4 (wax deposition with high inlet temperature: 50°C inlet, no heating, 20 mm wax layer) and Case 5 (wax deposition with low inlet temperature: 40°C inlet, no heating, 20 mm wax layer), representing the worst-case scenario). This chapter begins by describing the governing equations and boundary conditions used, followed by a step-by-step account of the simulation setup, model validation process, and data analysis techniques see Figure 5.

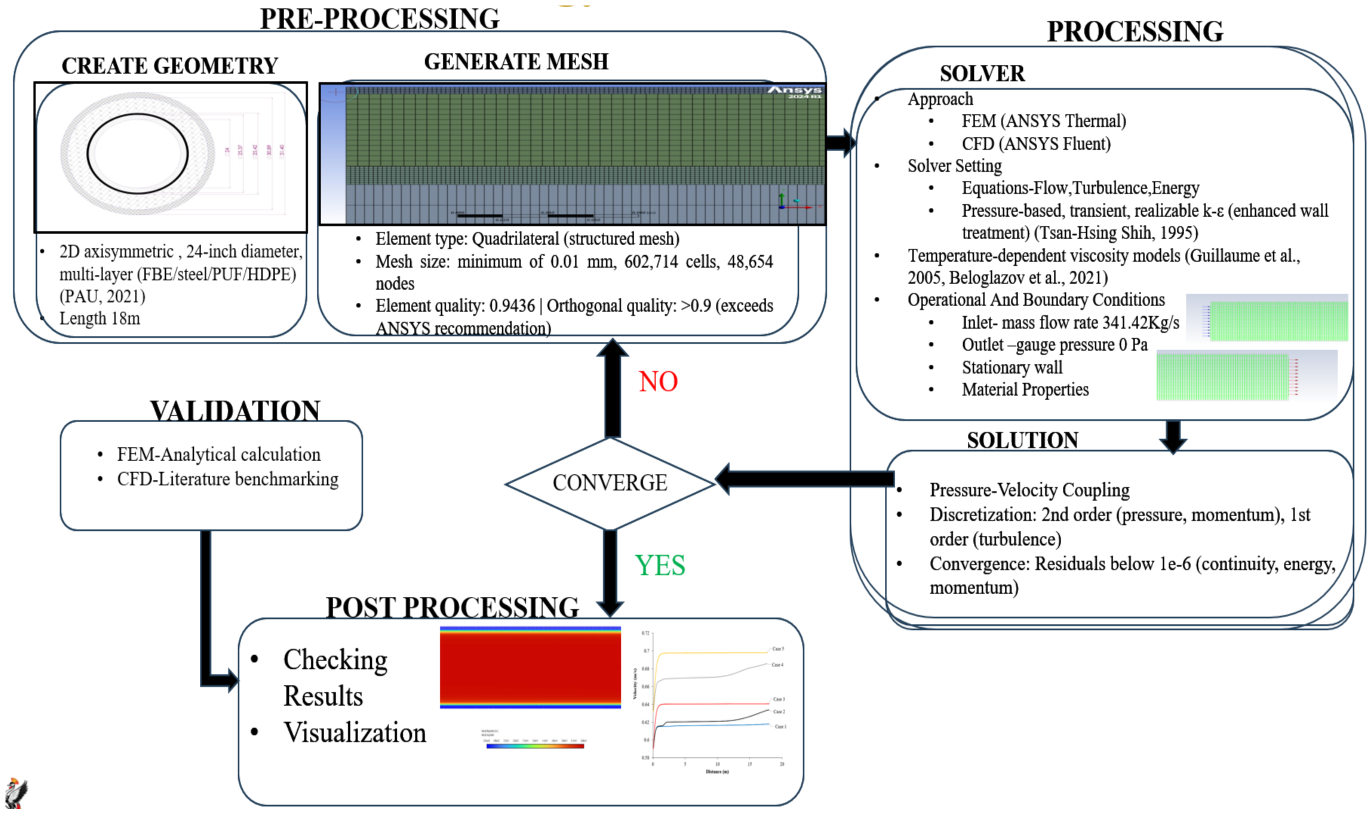

Figure 5: Flow chart showing the overall methodology

3.1 Modelling of the Cross-Section of the Pipeline

3.1.1 Geometry and Material Layers

The pipeline cross-section was modelled as a 2D axisymmetric geometry consisting of four concentric cylindrical layers as seen in Figure 6 and table 1, based on the EACOP design specifications (EACOP Ltd, 2022; PAU, 2021). The 2D axisymmetric assumption is valid because the pipeline is cylindrical and the flow and thermal conditions are symmetrical around the central axis. This approach significantly reduces computational cost while capturing the essential radial heat transfer physics (Lanzafame et al., 2017).

Table 1:Concentric cylindrical layers and their radius

Layer	Material	Inner Radius (m)	Outer Radius (m)	Thickness (m)
1	Crude oil	0	0.3048	0.3048
2	Steel pipe	0.3048	0.3112	0.0064
3	FBE	0.3112	0.3132	0.0020
4	PUF insulation	0.3132	0.4432	0.1300
5	HDPE casing	0.4432	0.4500	0.0068

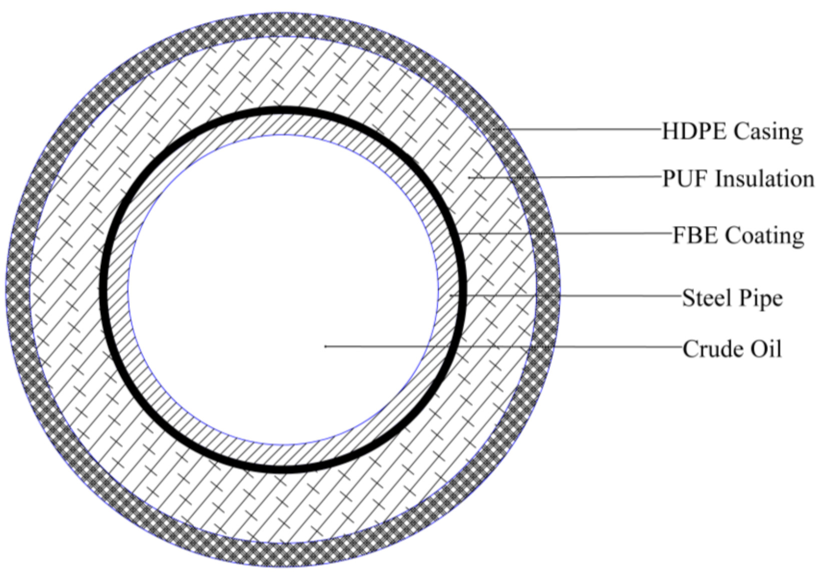

Figure 6: The different materials layers of the EACOP

3.1.2 Governing Equations for Heat Transfer

For steady-state radial conduction through a multi-layer cylinder, the heat transfer rate per unit length is given by Fourier's law applied to cylindrical coordinates (Yunus A. Cengel, 2016):

$$Q = \frac{2\pi k L (T_i - T_O)}{\ln{(r_o - r_i)}} \quad \text{Equation 3}$$

Where: Q is heat transfer rate (W), k is thermal conductivity of pipe wall (W/m·K), L is length of pipe segment (m), T_i is inner fluid bulk temperature (°C), T_O is outer soil temperature (°C), r_i is inner radius of pipe (m), r_o is outer radius of pipe including insulation (m).

For a multi-layer system, the total thermal resistance per unit length is the sum of the resistances of each layer as expressed by equation 4

$$R_{total}=R_{conv,in}+{}_{j=1}\sum{}_{n}2\pi k_j\ln(r_{j+1}/r_j)+R_{conv,out}$$ Equation 4

Where $R_{conv}=\frac{1}{2\pi rh}$ for convection at the inner and outer boundaries.

The corresponding heat flux at the external surface is given by equation 5:

$$q''=\frac{Q}{2\pi r_o L}$$ Equation 5

3.1.3 Partial-Fill Modelling

For partial-fill conditions (¾, ½, ¼ bore), the pipe cross-section contains both crude oil and stagnant air. The effective thermal resistance was calculated using a parallel resistance network:

Equation 6

$$\frac{1}{R_{EQ}}=\frac{A_{OIL}}{R_{OIL}A_{TOTAL}}+\frac{A_{AIR}}{R_{AIR}A_{TOTAL}}$$

A_{TOTAL} is full pipe cross-sectional area, R_{OIL}, R_{AIR} is thermal resistances of crude oil and air layers

Five different conditions of pipeline bore capacity were considered for the cross-sectional analysis namely: full bore of crude oil, three quarter full, halfway full, quarter full of crude oil and full bore of air as discussed below:

3.1.3.1 Full Bore Condition

When the pipeline is fully filled with crude oil, the conduction path is maximized due to oil-to- wall contact across the entire cross section. The governing equation reduces to radial conduction through the cylindrical wall which is given by equation 7.

$$q''_{full} = \frac{T_i - T_o}{\ln\left(\frac{r_o}{r_i}\right) / 2\pi k_{steel} L}$$ Equation 7

3.1.3.2 Three-Quarter Bore Condition

At 75% occupancy, crude oil occupies three-quarters of the cross-sectional area, while stagnant air fills the remaining quarter. The effective thermal resistance is recalculated using equation 8. The parallel resistance model, where oil conduction dominates but is weakened by the insulating air layer.

$$R_{eq} = \left(\frac{0.75}{R_{oil}} + \frac{0.25}{R_{air}}\right)^{-1}$$ Equation 8

Heat flux is then evaluated with R_{eq} incorporated into the radial conduction formulation.

3.1.3.3 Half Bore Condition

At 50% occupancy, the conduction pathway is evenly shared between crude oil and air, resulting in higher equivalent thermal resistance compared to the three-quarter bore case can be defined by equation 9.

$$R_{eq} = \left(\frac{0.5}{R_{oil}} + \frac{0.5}{R_{air}}\right)^{-1}$$ Equation 9

3.1.3.4 Quarter Bore Condition

With only 25% crude oil and 75% stagnant air, the dominant thermal resistance is from air. Consequently, the heat flux significantly decreases, indicating higher insulation effect due to air entrapment can be defined as equation 10.

$$R_{eq} = \left(\frac{0.25}{R_{oil}} + \frac{0.75}{R_{air}}\right)^{-1}$$ Equation 10

3.1.3.5 Full of air

When the pipeline is fully filled with air, the convective path is maximized due to air-to-wall contact across the entire cross section. The governing equation reduces to radial convection through the cylindrical wall given by equation 11.

$$R_{eq} = (\frac{1}{R_{air}})^{-1} \quad \text{Equation 11}$$

3.1.4 Assumptions for cross-sectional analysis

The cross-sectional FEM analysis was conducted under five key assumptions. First, steady-state heat transfer was assumed, which is appropriate for normal operating conditions where inlet temperature and heat trace power are constant. Second, all pipeline materials (API 5L steel, PUF, HDPE, and FBE) were treated as homogeneous and isotropic, following standard practice in pipeline thermal modelling. Third, contact resistance between adjacent layers was neglected because the layers are bonded during manufacturing (EACOP Ltd, 2022). Fourth, air in void spaces during partial-fill conditions was assumed stagnant, as natural convection in small annular gaps is minimal (Shoushtari et al., 2011). Fifth, thermal conductivities were taken as constant, since manufacturer data confirm that material properties are temperature-independent over the 18-70°C range relevant to this study.

3.2 Governing equations for the longitudinal analysis

This study adopted a set of governing equations to model the thermal-fluid behavior of crude oil within the EACOP. The physical processes are governed by the principles of conservation of mass, momentum, and energy. The fluid is assumed to be steady, incompressible, and Newtonian (crude oil temperature was above the pour point of 40°C), with temperature-dependent viscosity considered in the simulations. The equations are solved using Computational Fluid Dynamics (CFD) in ANSYS Fluent.

3.2.1 Conservation of Mass (Continuity Equation)

Mass conservation requires that fluid density and velocity satisfy the equation 12**.**

$$\frac{\partial \rho}{\partial t} + \nabla \cdot (\rho v) = 0 \quad \text{Equation 12}$$

where ρ is fluid density (crude oil density), t is time, and v is the velocity field. In practice, crude oil in the pipeline is often treated as incompressible (constant ρ), so the continuity equation simplifies to $\nabla \cdot v=0$, meaning the flow is divergence-free (no net mass accumulation). This ensures that the mass flow into any pipe segment equals the mass flow out.

3.2.2 Conservation of Momentum (Navier–Stokes Equation)

Momentum balance for a Newtonian fluid yields the Navier–Stokes equation. In vector form it is written as equation 13.

$$\rho(\frac{\delta v}{\delta t} + (v.\nabla)v) = -\nabla p + \mu \nabla^2 v + \rho g$$ Equation 13

where p is fluid pressure, μ is dynamic (shear) viscosity of the oil (Newtonian assumption), g is external body acceleration (such as gravity, often negligible for horizontal flow), ρ is the fluid density (density of crude oil).

The Navier Stokes equation represents inertia, pressure forces, viscous diffusion, and body forces such gravity, respectively. For internal pipe flow, this equation governs how pressure gradients and viscous stresses drive the velocity field. In component form (for x, y, z) it yields one equation per velocity component.

The viscous term $\mu \nabla^2 v$ arises from the Newtonian stress tensor. In a pipeline this equation captures the development of boundary layers at the walls and pressure-driven flow. Solving Navier–Stokes yields the velocity and pressure fields, which in turn determine the axial velocity profile.

3.2.3 Conservation of energy (Thermal energy equation)

Thermal energy conservation couples temperature with the flow. For an incompressible oil flow with heat conduction and viscous heating, a common form is defined in equation 14.

$$\rho C_P \left(\frac{\partial T}{\partial t} + v.\nabla T\right) = k\nabla^2 T + \varphi + Q$$ Equation 14

Where T is fluid temperature, c_p is specific heat at constant pressure, and k is thermal conductivity. The left side is the material (convective) derivative of temperature, while the right includes heat diffusion (first term), viscous dissipation Φ (often small), and any volumetric heat source Q. In a pipeline, a more detailed 1D energy balance is often defined as equation 15.

$$\rho A C_p \frac{\delta T}{\delta t} + \rho A C_p u \frac{\delta T}{\delta x} = \frac{\delta}{\delta x}\left(kA\frac{\delta T}{\delta x}\right) + Q_{fric} + Q_{ext} \qquad \text{Equation 15}$$

Where T is fluid temperature, c_p is fluid specific heat (constant-pressure heat capacity), k is fluid thermal conductivity (crude oil),u is axial velocity (the speed of oil in the pipe), Φ is viscous dissipation (conversion of shear into heat),Q is volumetric heat sources (heat trace).A is pipe area and u the axial velocity. Here the term Q_{fric} represents frictional (viscous) heating in the fluid, and Q_{ext} any heat flux through the pipe wall. In either form, the equation ensures that temperature changes arise from convective transport, conduction, and heat sources/sinks. This equation is used to predict how oil temperature evolves along the pipeline, including the effects of wall cooling/heating and viscous heating.

All governing equations are numerically solved in ANSYS Fluent using the finite volume method. Crude oil properties such as viscosity and thermal conductivity are defined as temperature-dependent using user-defined functions. Boundary conditions include specified inlet temperature and mass flow rate, while external surfaces of the pipe are subjected to convective heat transfer to simulate realistic field conditions

3.2.4 Turbulence Modelling

The realizable k-ε turbulence model was selected for this study. Unlike the standard k-ε model, the realizable variant incorporates a new formulation for turbulent viscosity and an improved transport equation for the dissipation rate (ε), enhancing its predictive capability for swirling flows, boundary layer separation and flows with strong streamline curvature. These characteristics are relevant to thermal fluid transport in pipelines (Tsan-Hsing Shih, 1995). The model is widely recommended for industrial applications involving heat and momentum transfer.

3.2.5 Temperature-Dependent Properties

Crude oil properties (density, viscosity, specific heat, thermal conductivity) were defined as temperature-dependent using piecewise linear interpolation based on PAU (2021) data (see Table 3.3). This is essential because viscosity, in particular, changes significantly with temperature (Mohyaldinn, 2019; Beloglazov et al., 2021).

3.2.5 Assumptions for CFD Analysis

The CFD modelling was done with the following assumptions: First the crude oil was treated as a Newtonian fluid as it was modelled at temperatures above the pour point (40°C); all simulated cases except Case 5 outlet remain above 40°C (Guillaume et al., 2005). Secondly the flow was considered incompressible flow as this is a standard for liquid pipeline flow. Thirdly a transient analysis was used as it captures thermal development along the 18 m section and fourthly negligible viscous dissipation was assumed as viscous heating is small compared to heat trace input (confirmed by initial sensitivity runs) and lastly no chemical reactions was assumed, the flow was treated as a single-phase flow; no wax precipitation modelled dynamically (assumed as fixed layer in Cases 4 and 5). A constant and uniform heat flux (70 °C heat trace) along the entire 18 m segment, as the control system maintains near-steady thermal conditions during steady-state operation

3.3 Modelling Protocol

3.3.1 Computing Environment

The simulations were conducted on a personal workstation running Windows 11 Pro 64-bit (Build 26100). The machine was equipped with an 11th Gen Intel(R) Core$^{(TM)}$ i5-11260H processor, featuring 20 physical cores operating at a base frequency of approximately 2.6 GHz. The system had 16 GB of DDR4 RAM installed, with 16.1 GB available to the operating system during computation. The workstation was manufactured by ASUS and operated with UEFI BIOS version NECN38WW. Graphics processing was managed through Microsoft Graphics Hybrid technology, with full support for DirectX 12. Although the system supported Miracast with HDCP, Mux switching was inactive during the simulations, and the discrete GPU remained the target device. This configuration provided sufficient computational performance and stability for the successful execution of the ANSYS simulations. The DirectX database version at the time of simulation was 1.7.2, and the system maintained standard DPI settings throughout the process following steps were followed during the modelling process.

3.3.1 Geometry preparation

The physical model of the pipeline, including multiple layers, was created using ANSYS Design Modeler. This step ensured accurate representation of the pipe geometry, capturing all structural and material layers. The two-dimensional geometry figure 7 of the pipeline was produced with ANSYS Design Modeler software. The length of the calculation domain is 18 m, and its diameter is 0.6096m /24 inches.

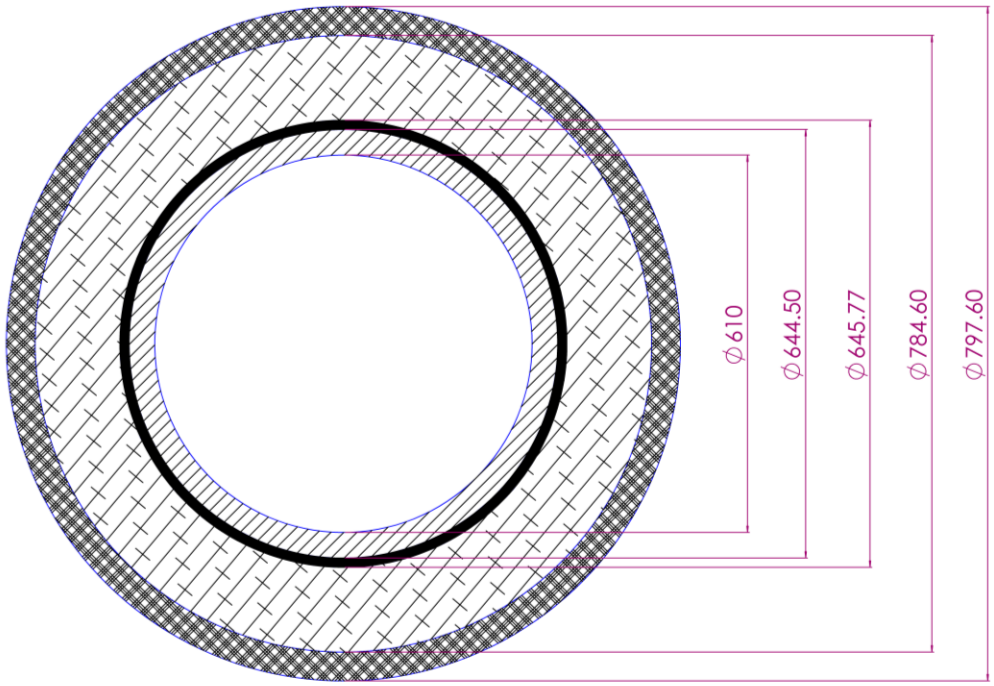

Figure 7: 2D cross section with dimensions

3.3.2 Preprocessing (meshing and set up)

The geometry was imported into ANSYS Meshing. The key domains such as inlet, outlet, wall boundaries, and fluid regions were defined. A structured mesh was generated to resolve the geometry with sufficient accuracy, ensuring proper element quality. The meshing of the 2D geometry has been done with Ansys Meshing software as seen in Figure 8, and the type of elements is structured. The computational domain was discretized using the quadrilaterals mesh to ensure uniformity and compatibility with complex geometries. The use of 40,500 quadrilateral cells ensured an adequate mesh resolution, with average orthogonal quality above 0.9, indicating reliable discretization. These conditions provide confidence in the validity of the simulation results.

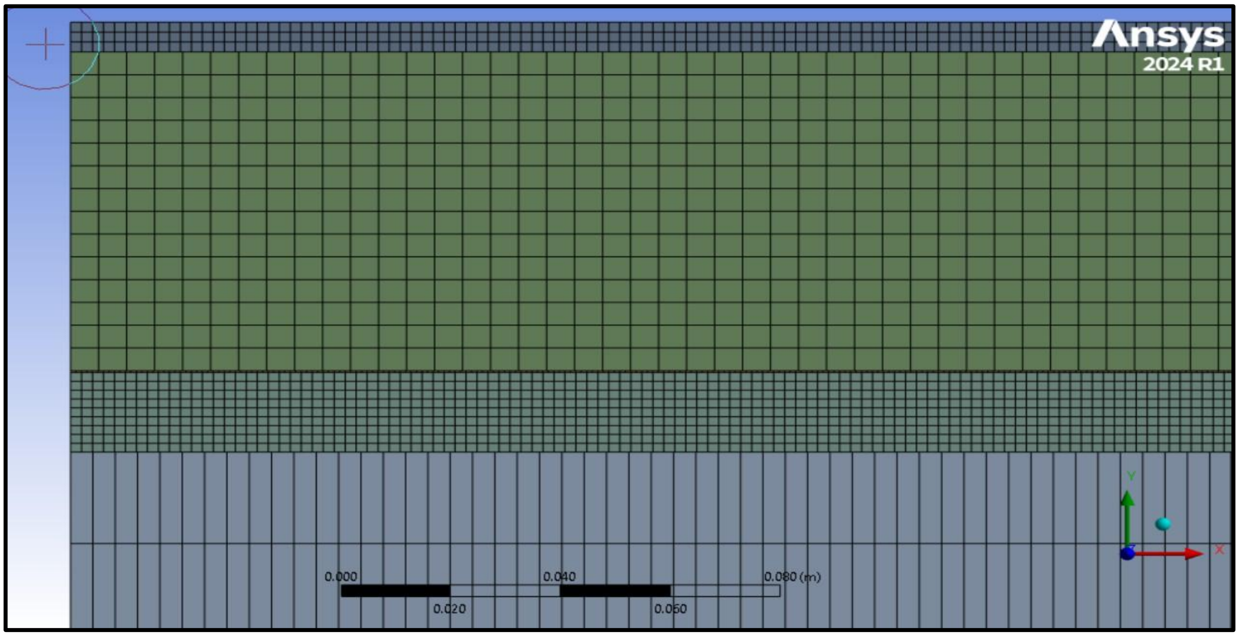

Figure 8: Different meshed layers

The element size was set to minimum of 0.01 m, providing a fine mesh suitable for capturing detailed flow and structural interactions. A total of 602,714 cells, 89,145 faces and 48,654 nodes were generated. The mesh quality metrics indicate a high-quality grid as shown in Figure 8**.** Average Element Quality was 0.9436 which suggests a well-shaped elements with minimal distortion as seen in figure 9 and figure 37 in Appendix. This mesh configuration strikes a balance between resolution and computational efficiency.

Skewness mesh metrics spectrum

Excellent	Very good	Good	Acceptable	Bad	Unacceptable
0-0.25	0.25-0.50	0.50-0.80	0.80-0.94	0.95-0.97	0.98-1.00

Orthogonal Quality mesh metrics spectrum

Unacceptable	Bad	Acceptable	Good	Very good	Excellent
0-0.001	0.001-0.14	0.15-0.20	0.20-0.69	0.70-0.95	0.95-1.00

© 2015 ANSYS, Inc. February 12, 2015

Figure 9: ANSYS Mesh Matrix Recommendation

3.3.3 Solution Setup (Physics and Boundary Conditions)

The meshed model was loaded into ANSYS Fluent. Table 2 provides a comprehensive summary of the numerical simulation setup implemented in ANSYS Fluent. It outlines the selected turbulence and viscous models, defined cell zone conditions for both fluid and solid domains, and the discretization schemes employed for pressure, momentum, and turbulence parameter.

Table 2: Simulation set up summary

Category	Parameter	Value
Turbulence Model	Viscous Model	k-ε (k-epsilon)
	Model Type	Realizable
Cell Zone Conditions	Fluid	Crude Oil
	Solids	FBE, HDPE, Polyurethane, Steel
Solution Methods	Pressure-Velocity Coupling	Coupled
	Pressure Discretization	Second-Order
	Momentum Discretization	Second-Order Upwind
	Turbulent Kinetic Energy Discretization	First-Order Upwind
	Turbulent Dissipation Rate Discretization	First-Order Upwind
Initialization	Method	Hybrid Initialization

Table 2 details the boundary and input conditions applied during the simulation. The specified inlet and outlet configurations, pressure conditions, and wall settings were established to ensure realistic representation of the operational flow environment within the pipeline system.

Table 3: Simulation inputs

Input parameters	Values
Pressure at outlet	Atmospheric pressure/gauge pressure
Inlet Type	Velocity Inlet
Inlet Mass flow rate	341.41 kg/s
Outlet Type	Pressure Outlet
Outlet Gauge Pressure	0 Pa
Walls	Stationary Wall

Table 3 presents the thermophysical properties of the working fluids incorporated into the computational model, namely paraffin wax, crude oil, and air. These parameters were integral to defining the flow behavior and heat transfer characteristics of the multiphase system.

Table 4: Fluid properties used in the simulation

Properties	Paraffin wax	Crude-Oil	Air
Density (Kg/M^3)	950	950	1.225
Cp (Specific Heat) (J/(Kg K))	2000	Piecewise Linear (2000-2400)	1006.43
Thermal Conductivity (W/(M K))	0.15	Piecewise Linear (0.15-0.156)	0.0242
Viscosity (Kg/(M S))	1	Piecewise Linear (0.000158-0.0007)	1.7894e-05
Molecular Weight (Kg/Kmol)	28.966	420	28.966
Pure Solvent Melting Heat (J/Kg)	150000		
Solidus Temperature (ºC)	35		
Liquidus Temperature (ºC)	45		

Table 4 summarizes the material properties assigned to the solid components of the pipeline assembly, including PUF, HDPE, steel, FBE and aluminum heat tracing. These properties were

used to characterize the thermal performance and structural response of the composite pipeline configuration.

Table 5: Solid properties used in the simulation

Properties	**PUF**	**HDPE**	**Pipe steel**	**FBE**	**Aluminum heat trace**
Density Kg/M^3	1250	965	7850	2200	2719
Cp (Specific Heat) J/(Kg K)	2100	2300	500	1800	871
Thermal Conductivity W/(M K)	0.028	0.4	50	0.3	202.4

The Fluent solver was executed using a realizable k-ε turbulence model with enhanced wall treatment under transient, pressure-based, and energy-enabled conditions. Residuals for continuity, velocity components, turbulence parameters, and energy all achieved convergence below the specified criteria, confirming numerical stability. Unlike the standard k–ε model, the realizable variant incorporates a new formulation for turbulent viscosity and an improved transport equation for the dissipation rate (ε), which enhances its predictive capability for swirling flows, boundary layer separation, and flows with strong streamline curvature all of which are characteristic of thermal fluid transport in pipelines like the EACOP. This model is widely recommended for industrial applications involving heat and momentum transfer (Tsan-Hsing Shih, 1995).

Crude oil was modeled as the working fluid since it reflects the actual operating conditions in the EACOP system. Its thermophysical properties were defined using typical values for Uganda's crude oil. The solid domain comprises Fusion Bonded Epoxy (FBE), polyurethane foam (PUF), HDPE casing, and API 5L X65 carbon steel. These materials represent the multilayer pipeline configuration used in the EACOP and are essential for modeling both conductive and convective heat transfer accurately across the pipeline wall and insulation layers.

The mass flow rate inlet condition was applied to define the inflow based on known 341.41 kg/s, representing the expected number of barrels per day in the EACOP pipeline. The Inlet Temperature is 50 °C that reflects the operational pre-heated temperature necessary to maintain crude oil fluidity. The Pressure Outlet (0 Pa) simulates ambient conditions at the receiving terminal, allowing the solver to compute the internal pressure distribution. All wall boundaries were treated as stationary to reflect buried and fixed pipeline conditions, eliminating wall motion effects and focusing on boundary layer development and thermal gradients.

Pressure Velocity Coupling Coupled Scheme was chosen for its superior stability and convergence in simulations with significant pressure-thermal interactions. Second-order discretization of pressure was used to improve accuracy in long-domain simulations. Second-order upwind scheme for momentum enhances resolution of velocity gradients and convective effects. First-order upwind discretization for turbulent kinetic Energy and dissipation was applied to ensure numerical stability during the early convergence phase.

Hybrid initialization was employed to provide a reliable initial solution using a combination of potential flow and mass-averaged conditions. This method is particularly effective for thermal fluid simulations where coupled fields (velocity and temperature) interact, improving convergence speed and stability. Initialization was performed and the solver was executed for transient analysis with the following assumptions were made during simulation.

(a) Crude Oil (Flow): During flow simulation along the pipe, crude oil is treated as a fluid.
(b) Crude Oil (Thermal Analysis): For heat transfer simulations across the pipe cross-section, crude oil is assumed to behave as a solid to model thermal conduction.
(c) A pressure-based solver was chosen due to the incompressibility of the flow.
(d) Simulation Type: The simulation is conducted as a transient analysis.
(e) Gravity: Gravitational acceleration is applied along the Y-axis with a value of –9.81 m/s^2.
(f) Meshing Assumption: The contact resistance between the pipe layers was assumed to be negligible during meshing.

The thermal fluid behavior was modelled and simulated in five case scenarios as summarized by Table 6.

Table 6: Summary of the five case scenarios for the thermo fluid behavior

INPUT				OUTPUT		
Inlet temperature (^{0}C)	**Source heat (^{0}C)**	**Ambient temperature (^{0}C)**	**Wax thickness (mm)**	**Temperature profile**	**Velocity profile**	**Viscosity profile**
Case 1 *(Base Case with External Heating): To establish the baseline behavior with active heating and analyze its impact on preventing thermal losses and viscosity changes*						
50	**70**	**25**	**0**	**-**	**-**	**-**
Case 2 *(Base Case without Heating): To isolate the effect of heat loss to the environment by comparing with Case 1*						
50	**None**	**25**	**0**	**-**	**-**	**-**
Case 3 *(Reduced Inlet Temperature): To investigate the sensitivity of the flow to a lower inlet temperature, focusing on its impact on cooling rate and viscosity*						
40	**None**	**25**	**0**	**-**	**-**	**-**
Case 4 (*Wax Deposition (High Inlet Temp)): To analyze the impact of wax deposition on flow hydraulics and thermal performance, starting from a higher inlet temperature*						
50	**None**	**25**	**20**	**-**	**-**	**-**
Case 5 (*Wax Deposition (Low Inlet Temp)): To study the compounded effect of wax deposition and a lower inlet temperature, representing a more severe operational scenario*						
40	**None**	**25**	**20**	**-**	**-**	**-**

3.3.3 Post process the results

Simulation results were analyzed using ANSYS Fluent and CFD-Post Temperature, Velocity and viscosity distributions along the pipeline were visualized. The influence of parameters on thermal performance was studied. Critical areas with significant temperature gradients or thermal stress were identified for further evaluation. A comparison with Analytical results was done to valid model results.

3.3.4 Justification of modelling Choices

A two-dimensional axisymmetric model was selected to significantly reduce computational cost while capturing the essential physics of radial heat transfer and axial flow. This approach is valid because the pipeline is cylindrical and the flow and thermal conditions are symmetrical around the central axis, a common and validated simplification in pipeline studies (Lanzafame et al., 2017).

The model explicitly includes all key insulation layers that’s to say the steel pipe, Fusion Bonded

Epoxy (FBE) coating, Polyurethane Foam (PUF) insulation, and the High-Density Polyethylene (HDPE) outer casing. Their thermal properties (conductivity, specific heat) are critical inputs, making the heat loss calculations realistic.

The inlet temperatures of 50°Cand 40°C were selected to be safely above the crude's pour point (40°C). The soil temperature ranges represent a typical average for the region (Banage, 1967). The mass flow rate of 341.41 kg/s corresponds to the designed throughput of 216,000 barrels per day, ensuring the simulation reflects actual operational conditions.

The modelling length of 18 m is the standard length of a single pipe segment used in the EACOP before welding (EACOP Ltd, 2022). Modelling one segment allows direct comparison with segment-level thermal and hydraulic behavior thus this gives a practical correspondence. For boundary layer development, the thermal and hydrodynamic entry lengths for crude oil flow at Re ~ 5,000-10,000 are typically between 5 and 15 m. An 18 m domain ensures that both the velocity profile and the temperature profile become fully developed before the outlet, avoiding entry-length artefacts. And for computational feasibility, the full 1,443 km transient CFD simulation is not practical with current desktop resources. The 18 m segment provides a computationally efficient yet physically representative domain that captures the essential radial and axial gradients.

3.3.5 Scaling of the 18 m Results to the Full Pipeline Length

While an 18 m segment is adequate to capture local thermo-fluid behavior, the EACOP extends over 1,443 km. Four complementary methods are proposed to extrapolate the 18 m segment results to the full pipeline length.

3.3.5.1 Quasi-1D Bulk Energy Balance

The dominant axial temperature variation is governed by the one-dimensional energy equation as seen in equation 16 below for the bulk fluid (Yuan Q, 2023):

$$\rho Q C_p \frac{dT_b}{dx} = \frac{-2}{R} U(T_b - T_{soil}) \qquad \text{Equation 16}$$

U is the overall heat transfer coefficient derived from the validated 2D FEM cross-sectional model,

R the inner pipe radius, ρ the density, Q the volumetric flow rate, C_p the specific heat capacity, $T_b$the bulk fluid temperature, and $T_{soil}$the ambient soil temperature. This ordinary differential equation can be integrated over the full pipeline length using a segment-averaged

U value, giving the temperature drop over the entire route. The 1D energy balance is widely used for long-distance buried hot oil pipelines because it preserves the essential physics while drastically reducing computational cost (Modisette, 2016).

3.3.5.2 Sequential (Segment-Marching) Boundary Conditions

The pipeline is divided into contiguous 18 m segments. The outlet conditions (temperature, velocity, viscosity profiles) of one segment serve as the inlet conditions for the next segment – an approach known as the segment-marching method (OpenModelica, 2021). Because the flow is fully developed at the end of each 18 m segment, only the bulk values need to be passed, making the algorithm computationally efficient. This method is equivalent to a quasi-1D marching scheme and is standard practice in pipeline thermal design (Modisette, 2016).

3.3.5.3 Linear Pressure Drop Scaling

For fully developed laminar flow in a constant-diameter pipe, the pressure drop scales linearly with length according to the Hagen-Poiseuille equation (White, 2016):

$$\Delta P = \frac{8\mu LQ}{\pi R^4}$$ Equation 17

For the normal heated operation of the EACOP (Case 1), where the viscosity remains nearly constant, the total pressure drop over the full pipeline is obtained by scaling the segment-wise pressure drop:

$$\Delta P_{total} = \frac{L_{total}}{18} \times \Delta P_{18\,m}$$ Equation 18

For failure scenarios where viscosity increases significantly along the pipe, a refined segment-wise approach is required: the outlet viscosity of each segment is used to compute the pressure gradient for the next segment, accounting for the progressive viscosity rise.

3.3.5.4 Periodic Thermal Development for Heated Operation

Under normal heated operation (Case 1), the thermal development length for the EACOP is estimated to be less than 500 m. Beyond that distance, the temperature profile becomes periodic: the heat input from the trace balances the heat loss to the soil, and the temperature repeats every segment (Yang et al., 2021). Therefore, after the first 30 segments (~540 m), the full-pipeline temperature can be approximated by repeating the 18 m segment results with periodic boundary conditions. This periodic assumption is common in long-distance heated pipeline simulation and dramatically reduces computational effort.

CHAPTER FOUR: RESULTS AND DISCUSIONS

This chapter presents a comprehensive analysis of the thermal-fluid behavior of the heated crude oil in the EACOP under a range of operational and abnormal conditions. The findings are synthesized to interpret trends in temperature distribution, heat loss, and fluid flow behavior, with the aim of translating numerical results into actionable insights for pipeline design, operation, and risk management.

The results and discussions are structured into two main sections: cross-sectional modeling which addresses specific objective 1 and longitudinal analysis which addresses the specific objective 2 and 3. The cross-sectional modeling focuses on temperature distribution across the pipeline's cross section, heat transfer dynamics at varying fill levels, and the influence of ambient soil temperature on radial heat loss. The longitudinal analysis examines thermal-fluid behavior along the pipeline under five case scenarios, simulating both normal operations and heat trace failure events. In each scenario, velocity, temperature, and viscosity profiles are evaluated along the pipeline length and across its cross-section.

4.1 Results for Objective 1: Cross-Sectional Heat Loss

The specific objective one was to design and simulate a FEM model of radial heat loss across the cross section of the pipe for different crude oil fill levels (at full, three quarter, half and quarter filled) and ambient temperatures (18°C to 35°C).The results for this objective is categorized as the cross sectional heat loss which is made of the temperature distribution across the cross-section of the pipeline, the cross sectional heat transfer analysis at different fill level of the pipe and the effect of varying soil ambient temperature on heat loss and these are discussed below:

4.1.1 Results for temperature distribution across the cross section of the pipeline

The temperature distribution across the cross section of the pipe in figure 10 shows a steady-state thermal analysis of a heated pipeline cross-section with temperature distribution across the pipe wall and surrounding insulation. The temperature gradient ranged from a minimum of 25°C to a maximum of 70 °C. The inner core, representing the crude oil, exhibited a relatively uniform temperatures between 50°C and 60°C, indicating effective heat transfer into the fluid. The highest temperatures are localized near specific regions of the outer wall, as shown by the red hotspots, corresponding to heating trace raceways. The coolest regions were found at the outermost edge of the insulation the HDPE layer, demonstrating the thermal gradient across the pipe thickness. The

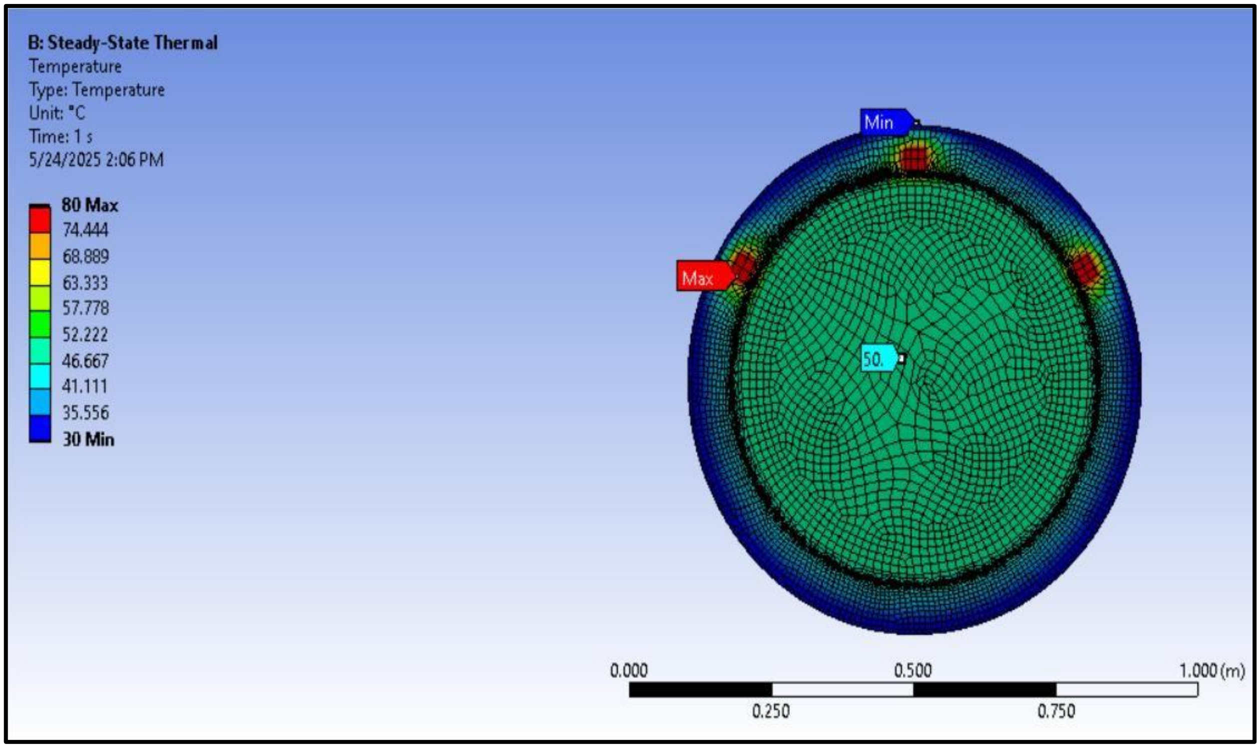

Figure 10: Steady state Temperature distribution across the cross section of the pipe

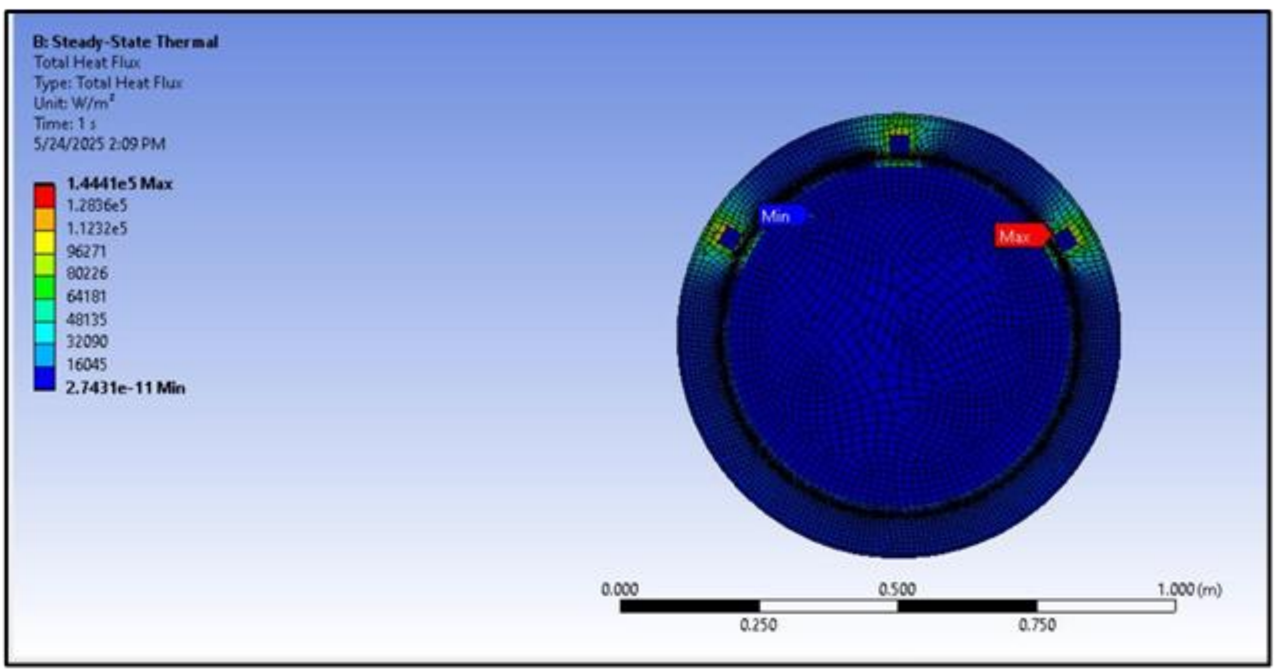

Figure 11: Heat flux across the cross section with heating

Figure 11 illustrates the total heat flux distribution across the cross-section of a heated pipeline from a steady-state thermal analysis of a no heating scenario. The maximum heat flux reaches approximately 1.444×10^5 W/m², primarily concentrated around localized regions near the outer insulation layer, as highlighted in red. These hotspots suggest the presence of concentrated thermal gradients, due to heat sources that enhance local heat transfer. In contrast, the interior of the pipeline representing the fluid domain exhibits minimal heat flux values, with the lowest recorded at nearly 2.74×10^{-11} W/m², indicating negligible conductive resistance within the fluid region due to uniform internal heating. The results validate that the outer insulation plays a crucial role in thermal containment, with the majority of the heat flux being dissipated at the boundary, thus effectively preserving internal thermal conditions essential for maintaining crude oil viscosity and flow performance.

The steady-state temperature distribution across the pipeline cross-section confirms the effectiveness of the integrated insulation and heating system. The presence of a relatively uniform, high-temperature core (50-60°C) surrounded by a significant thermal gradient through the insulation layers is a demonstration of controlled heat transfer. The localized hotspots at the heating trace raceways are expected and indicate zones of active energy input, while the cool outer HDPE surface demonstrates successful thermal containment, minimizing energy loss to the environment.

The remarkably low heat flux values recorded within the fluid domain (as low as $\sim10^{-11}$ W/m²) are highly significant. This does not indicate "negligible conductive resistance" but rather points to a state of near-thermal equilibrium within the crude oil bulk during steady-state operation. This uniformity is critical, as it prevents the formation of cold spots on the pipe wall where wax deposition typically initiates. The high heat flux at the insulation boundary underscores its role as the primary thermal barrier; the system is designed such that the most intense thermal gradients occur within the insulation itself, protecting the fluid from the ambient environment.

4.1.2 Cross-sectional heat transfer analysis at different fill levels

Numerical modelling was performed to estimate heat transfer across the pipe cross-section at four fill conditions: full bore, three quarter, half, and quarter full. The crude oil was assumed at 50°C with the surrounding soil at 25°C. The temperature distribution for a pipe full of crude oil is shown in the figure 12 showing temperatures ranging from 50°C in the pipe and 25°C on the outer layer of the insulator and HDPE casing.

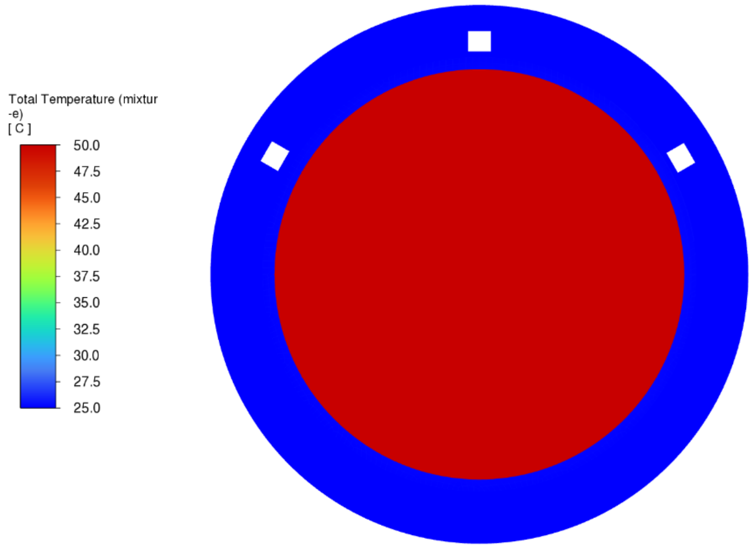

Figure 12: Temperature distribution of a full-bore pipe of crude oil

The temperature distribution of the half bore full pipe with crude oil is shown by the contour plot below in figure 13, for the half bore full is shown in figure 14 and the quarter full pipe bore is shown in the figure 15.

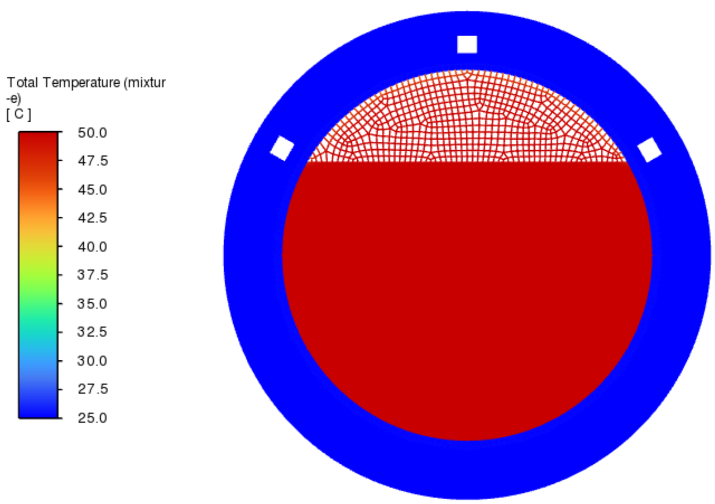

Figure 13: Temperature across the cross section of a three-quarter full-bore pipe

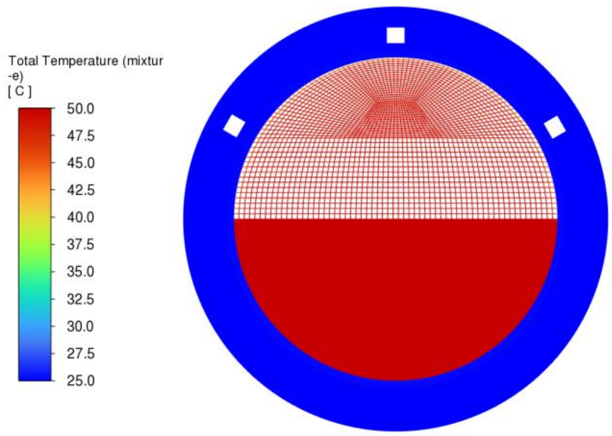

Figure 14:Temperature across the cross section of a half full bore pipe

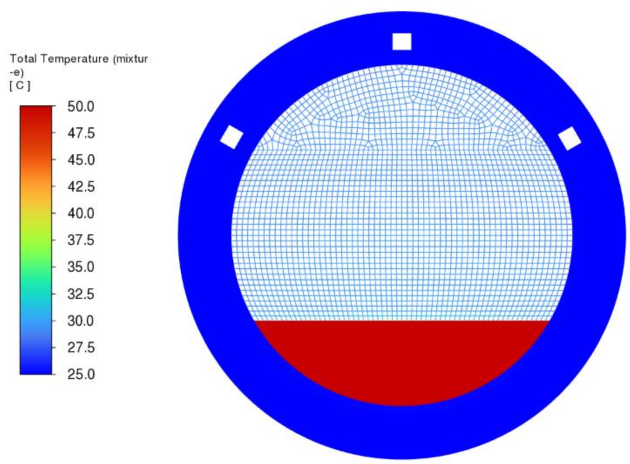

Figure 15: Temperature across the cross section of a quarter full bore pipe

The heat transfer rates were approximately (-1.69×10^{-11} W) identical across four cases of full bore with crude oil, three quarter full, half and quarter full bore of crude oil while with full bore of air the heat transfer rate was approximately $-7.36\text{x}10^{-12}$ W as seen in figure 16**.**

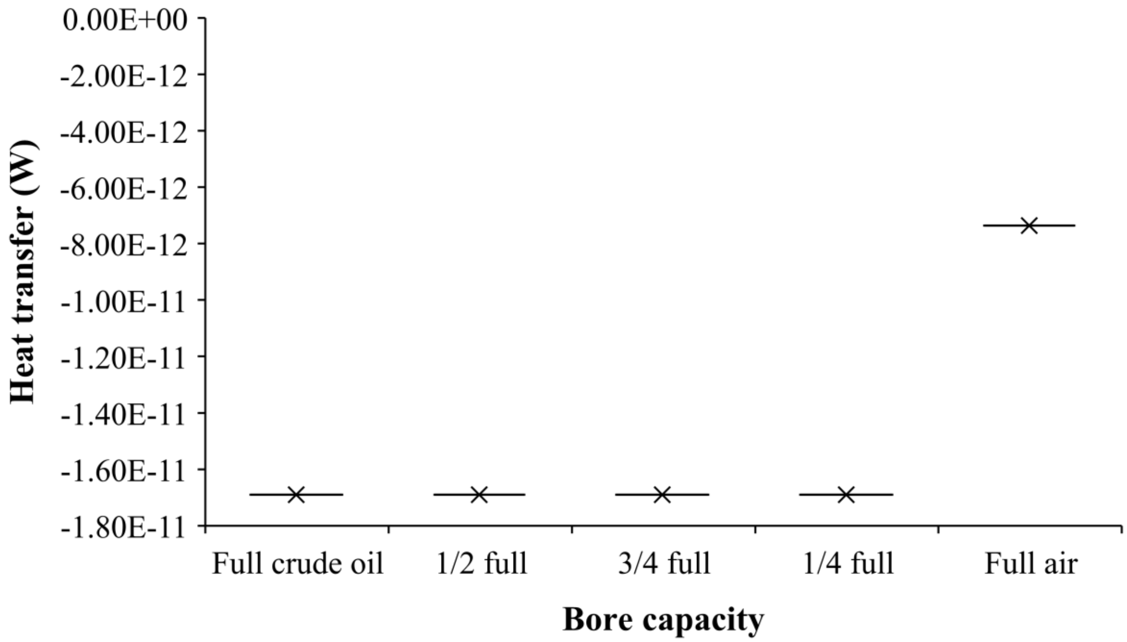

Figure 16: Heat transfer against Bore Capacity

The analysis of varying fill levels yielded an insightful result: the heat transfer rate was approximately identical (-1.69×10^{-11} W) for all conditions containing crude oil (full, 3/4, 1/2, 1/4 bore). This strongly suggests that the dominant thermal resistance in the system is not the convective heat transfer within the fluid, but the conductive resistance of the pipeline wall and insulation layers. As long as the fluid is present and in contact with the pipe wall, the heat loss pathway remains largely unchanged. The drastically lower heat loss for the air-filled case (-7.36×10^{-12} W) further supports this, as air has a much lower thermal conductivity and capacity than crude oil, fundamentally altering the heat transfer mechanism. This finding implies that during transient operations like shutdowns and restarts, the fill level may become a critical factor as the heat loss in a pipe full of air shows 56% lower heat loss because air has lower thermal conductivity, but during steady-state flow, the insulation system dictates the heat loss rate. Cengel et al., 2016 provides clear tables and discussions on the thermal conductivity of various fluids. It states that the thermal conductivity of air (0.026 W/m.K) is lower than that of liquids like oil (0.15 W/m.K) and the above results demonstrates this property.

4.1.3 The effect of ambient soil temperature on radial heat loss

A cross-sectional analysis was conducted to quantify the radial heat loss from the pipeline under a constant crude oil temperature of 50°C, simulating a steady-state operating condition. The ambient soil temperature was varied from 18°C to 35°C to investigate its effect on the thermal performance of the pipeline. The results, summarized in Table 7 and illustrated by figure 17, demonstrate a clear and direct relationship between the environmental conditions and the system's heat loss (Cengel et al., 2016).

Table 7: Radial heat loss at varying soil temperatures

Inner Temperature (°C)	**Soil Temperature (°C)**	**Heat Loss, Q (W/m)**
50	18	-5,257
50	20	-5,054
50	25	-4,547
50	30	-4,040
50	35	-3,533

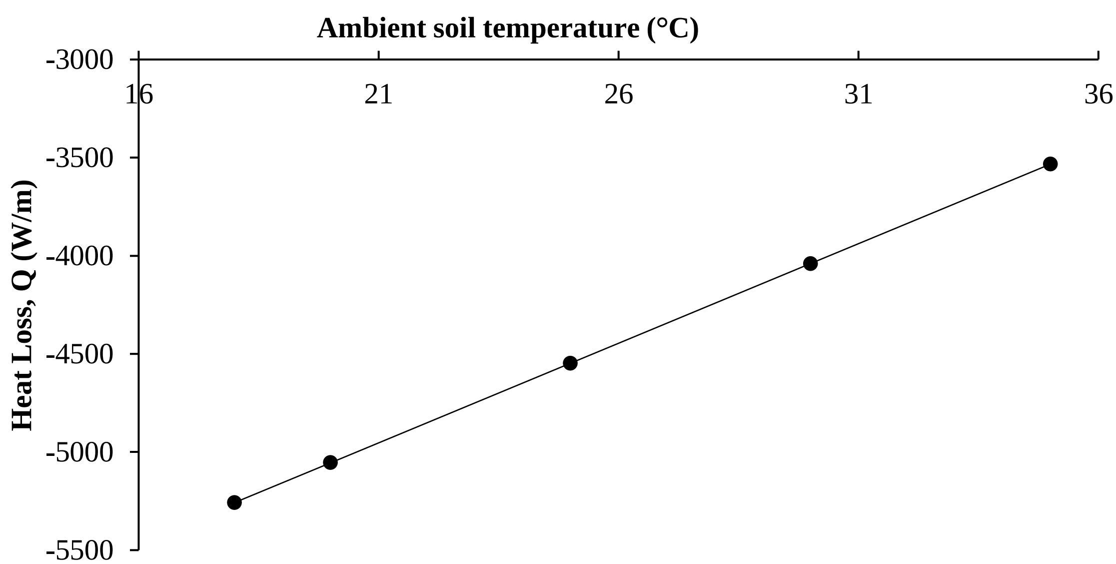

Figure 17: Heat loss against soil temperature

The data reveals that the radial heat loss, denoted by the negative value of Q indicating energy leaving the system, decreases as the soil temperature increases. Specifically, when the soil temperature was raised from 18°C to 35°C, the heat loss decreased by approximately 32.8%, from

-5,257 W/m to -3,533 W/m in figure 17. This trend is attributed to the reduction in the thermal driving force the temperature difference (ΔT) between the crude oil and the surrounding soil. As the ambient condition becomes warmer, the rate of heat transfer from the pipeline to the soil is reduced.

This finding has significant practical implications for the operational planning of the EACOP. The substantial variation in heat loss underscores that the thermal demand on the pipeline's heating system is not constant but is highly dependent on local and seasonal ground temperatures.

Consequently, sections of the pipeline traversing cooler regions or operating during colder seasons will require significantly greater energy input to maintain the crude oil temperature above its critical wax appearance point, directly impacting operational costs and energy consumption.

4.2 Results for Objective 2&3: The thermal fluid behavior along the pipeline

This section presents the results of specific objective two and three where five cases were simulated using computational fluid dynamics (CFD) to investigate the thermo-fluid dynamic behavior within an 18-meter pipeline section of the EACOP pipeline under different operational and boundary conditions. These results showed the individual and combined effects of inlet temperature, external heating, and wax deposition on the temperature, velocity, and viscosity profiles. The results are divided into contour plots of temperature, velocity and viscosity for each of the five cases and a comparative analysis of temperature, velocity and viscosity for all the five cases:

4.2.1 Contour Plots of temperature, velocity and viscosity

These contour plots give visual representation of how a scalar quantity of temperature, velocity magnitude and molecular viscosity vary across the computational domain. The ANSYS software discretizes the domain into small elements (cells) and assigns a color to each region according to the local value of the chosen variable. These Contour plots assist in rapidly interpreting the results of CFD simulations allowing for identification of spatial trends and detection of critical regions. Below are the contour plots for each of the five cases

4.2.1.1 Contour plots of temperature, velocity and viscosity for Case 1

The temperature contour under heating condition below in figure 18, shows oil temperature being maintained closer to the inlet value along the length of the pipeline. The crude oil core is thermally uniform radially, while the insulation layers show a gradient, confirming thermal containment.

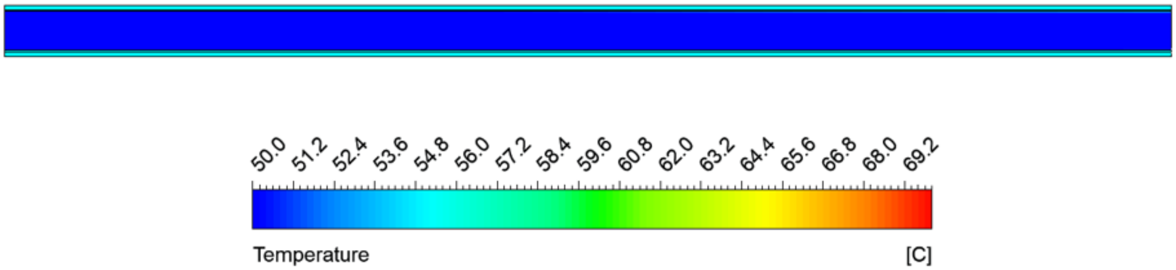

Figure 18: Temperature contour for Case 1

The velocity contour shown by figure 19 presents the velocity contour along the pipeline section for Case 1 (normal heated operation: 50°C inlet, 70°C heat trace). The velocity scale ranges from 0 m/s (dark blue) at the pipe wall to approximately 0.52 m/s (dark red) at the pipe centerline. The contour exhibits a parabolic velocity profile characteristic of laminar or transitional pipe flow. Velocity is zero at the pipe wall (no-slip condition) and increases progressively toward the centerline, reaching a maximum of approximately 0.52 m/s. The profile is symmetric about the centerline, confirming that the flow is fully developed and free from asymmetric disturbances.

Along the pipe length from 0 m to 18 m, the velocity increases gradually from approximately 0.50 m/s at the inlet to 0.52 m/s at the outlet. This mild acceleration is attributed to the reduction in fluid viscosity as the crude oil is heated by the 70°C heat trace (as shown in the temperature contour). Lower viscosity reduces flow resistance, allowing the same pressure gradient to produce higher velocities.

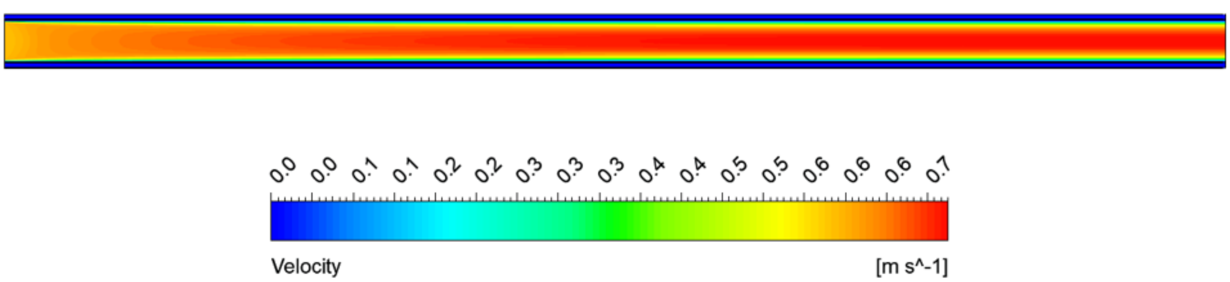

Figure 19: Velocity contour for Case 1

The contour plot of molecular viscosity, presented in figure 20 below, shows a uniform viscosity field across the entire domain, with no radial or axial variation. The viscosity remains constant at approximately 0.158 kg/(m·s) from the inlet (0 m) to the outlet (18 m) and from the pipe centerline to the wall. This uniformity confirms that the crude oil is isothermal under active heating, as temperature is the primary determinant of viscosity for waxy crude oils. The absence of viscosity gradients indicates that the active heating system (70°C heat trace) successfully balances heat loss to the surrounding soil, maintaining a constant fluid temperature. The constant, relatively low viscosity (0.158 kg/(m·s)) corresponds to minimal flow resistance, representing the optimal pumping condition for the EACOP.

`

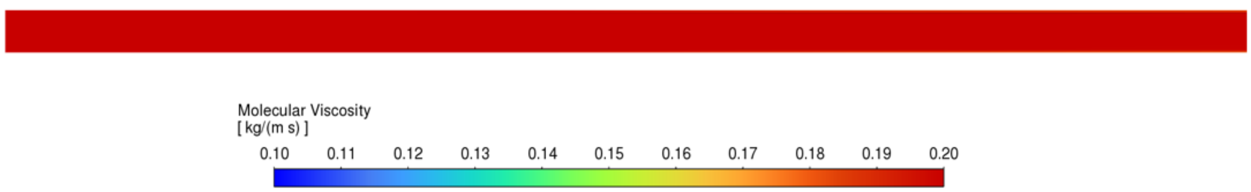

Figure 20: Viscosity contour for case 1

4.2.1.2 Contour plots of temperature, velocity and viscosity for Case 2

Temperature contour shown in figure 21 below presents the steady-state temperature contour along the pipeline section under a no-heating scenario. As the fluid travels downstream without active heating, the core temperature decreases progressively due to heat loss to the surrounding soil. By the outlet, the core temperature has dropped to approximately 45–46°C. A radial temperature gradient is evident across the pipe cross-section at each axial position. The crude oil near the pipe wall is cooler (green to blue, 30–40°C) than the core due to conductive heat transfer through the wall and insulation. This wall cooling increases the risk of wax deposition, as the wall temperature may fall below the wax appearance temperature even if the bulk temperature remains above the pour point. The temperature decreases further across the insulation layers, reaching approximately 25°C (blue) at the outer HDPE casing, which is in contact with the soil. The steep gradient within the insulation confirms that the polyurethane foam (PUF) layer provides significant thermal resistance, but without active heating, heat loss is unavoidable.

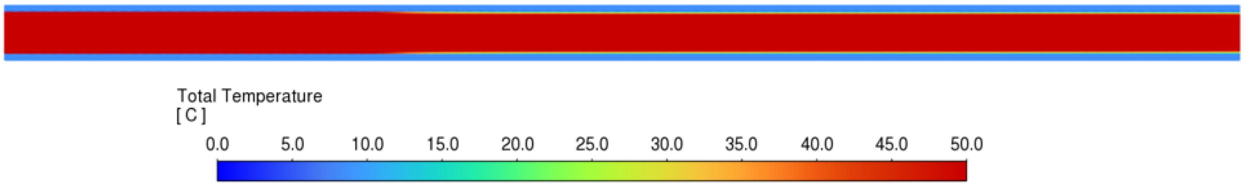

Figure 21: Temperature contour for Case 2

Velocity contour in figure 22 shows velocity magnitude along the pipeline section for a no-heating scenario. The contour exhibits a parabolic velocity profile characteristic of laminar or transitional pipe flow. Velocity is zero at the pipe wall (no-slip condition) and increases toward the centreline, reaching a maximum of approximately 0.73 m/s. This maximum is higher than in the heated case (0.52 m/s) because the crude oil is cooler and more viscous; to maintain the same mass flow rate, the pressure gradient increases, which in turn produces a higher centreline velocity for a given flow area. Along the pipe length, the velocity increases gradually from approximately 0.48 m/s at the inlet to 0.51 m/s at the outlet. This mild acceleration (≈6%) is due to the combined effect of the imposed pressure gradient and the slight cooling-induced viscosity increase, which alters the velocity profile shape while conserving mass. The profile remains symmetric and fully developed, with no flow separation or recirculation. The absence of near-wall stagnation zones indicates that, even without active heating, the flow remains stable over the 18 m section. However, the lower near-wall velocities (dark blue band) are broader than in the heated case, reflecting the higher viscosity fluid's resistance to shear near the boundary.

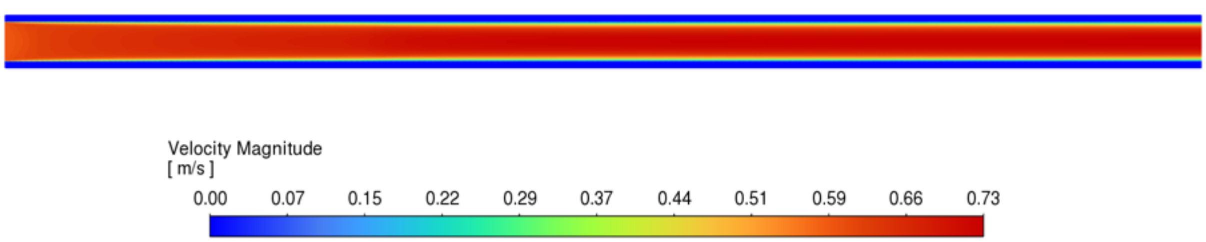

Figure 22: Velocity contour for Case 2

Viscosity Contour in figure 23 presents the molecular viscosity contour along the pipeline section for a no-heating scenario. As the fluid travels downstream without active heating, heat loss to the surrounding soil causes the temperature to decrease. Consequently, the viscosity increases progressively along the pipe, at the outlet. A radial viscosity gradient is evident at each axial position. The fluid near the pipe wall is cooler than the core due to conductive heat loss through the insulation, resulting in higher viscosity near the wall compared to the centreline. This near-wall viscosity increase is critical for flow assurance because it reduces the effective flow area and increases frictional pressure drop.

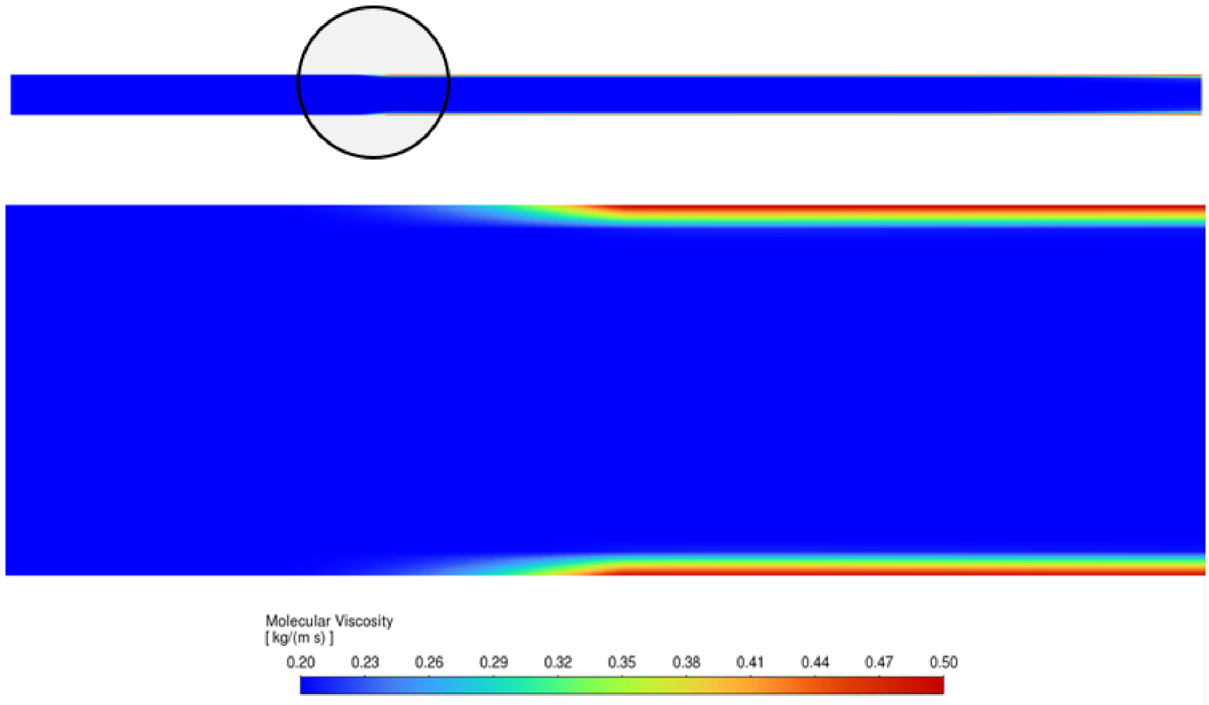

Figure 23: Viscosity contour for Case 2

4.2.1.3 Contour plots of temperature, velocity and viscosity for Case 3

Temperature contour in figure 24 shows a radial temperature gradient is present at each axial position. The fluid near the pipe wall is cooler than the core due to conductive heat transfer through the insulation and into the soil. Near-wall temperatures are well below the pour point and also below the wax appearance temperature, creating conditions highly favorable for wax nucleation and deposition. The temperature decreases further across the insulation layers, the steep gradient within the PUF layer confirms its thermal resistance, but without active heating, the heat loss is unavoidable and rapid. The entire crude oil domain beyond the immediate inlet region contains fluid at or below the pour point.

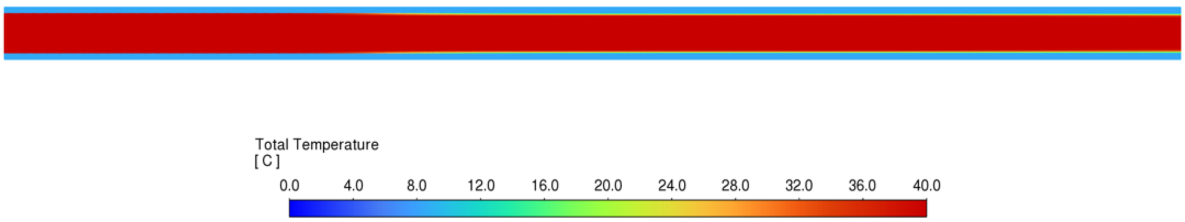

Figure 24: Temperature contour on Case 3

Velocity contour shown in figure 25 reveals a parabolic velocity profile characteristic of laminar or transitional flow, but with a flatter centerline region compared to the 50°C no-heating case. The near-wall velocity gradient is steeper than in heated cases because the high-viscosity fluid adheres strongly to the wall (no-slip condition) and the velocity rises sharply over a thin boundary layer. This steep gradient increases wall shear stress and frictional pressure drop, directly raising pumping power requirements. The velocity field remains symmetric and attached, with no recirculation, indicating that even under this severe cooling, the flow does not separate.

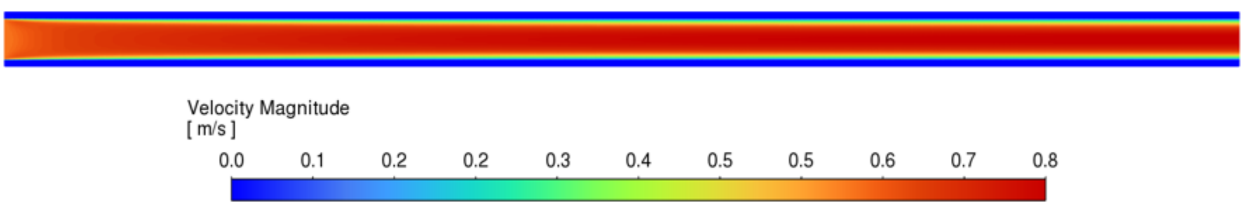

Figure 25: Velocity contour in Case 3

Viscosity contour in figure 26 shows a radial viscosity gradient with the fluid near the pipe wall having higher viscosity than the core. This gradient results from the radial temperature gradient: the near-wall fluid is cooler (as shown in the temperature contour for this case) and therefore more viscous. The elevated near-wall viscosity increases wall shear stress and frictional pressure drop, directly raising pumping power requirements. The uniformly high viscosity across the entire domain (all values > 0.496 kg/(m·s)) indicates that the crude oil is well above its normal operating viscosity and is at significant risk of wax deposition and flow instability.

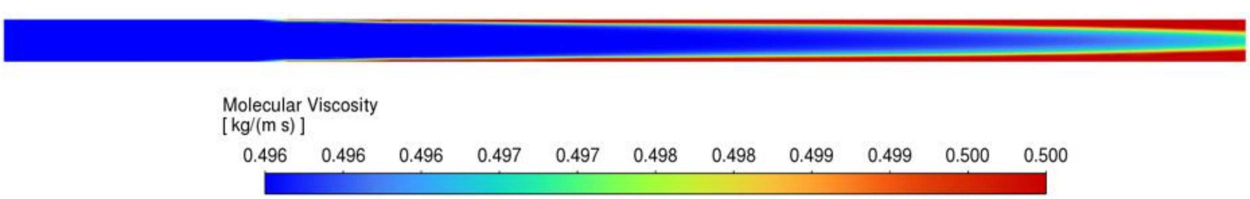

Figure 26: Viscosity contour for Case 3

4.2.1.4 Contour plots of temperature, velocity and viscosity for Case 4

Temperature contour in figure 27 shows the wax layer acts as a partial insulator, which can be seen as a modified thermal boundary. However, the geometric constriction, does not change the core fluid's cooling rate from the 50°C inlet.

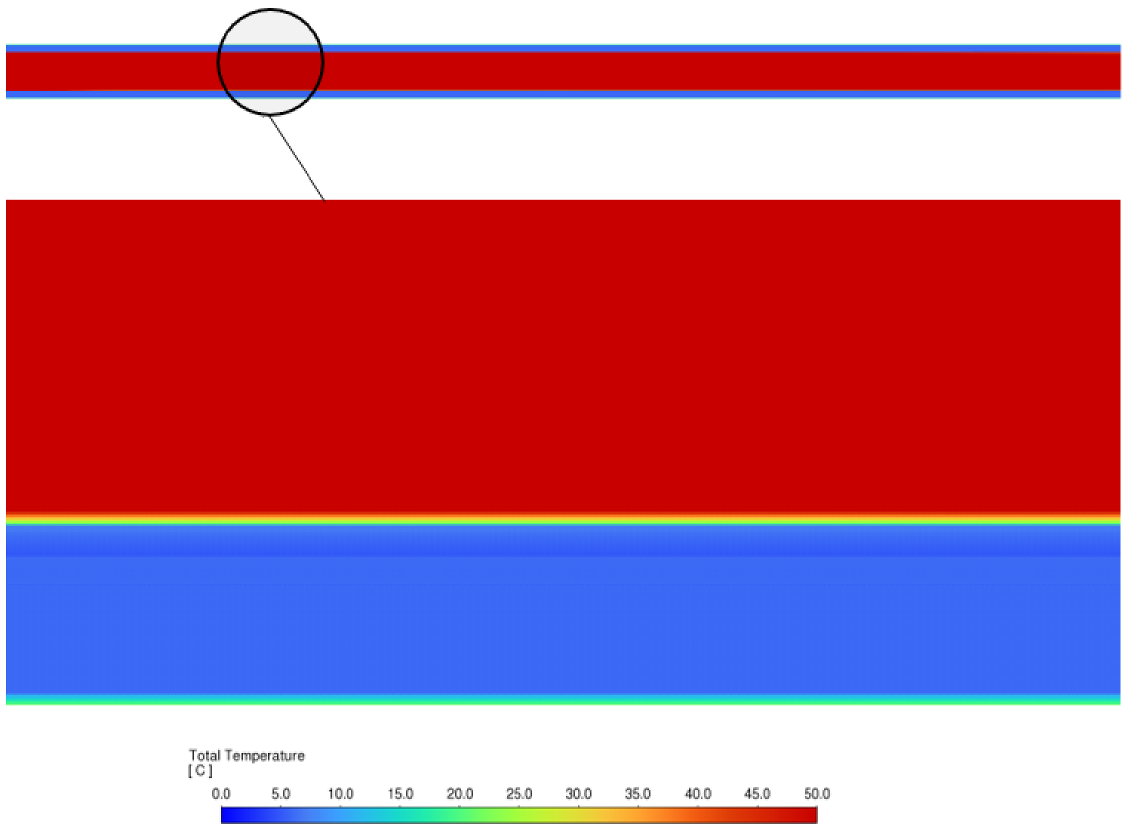

Figure 27: Temperature contour for Case 4

Velocity contour in figure 28 clearly shows the impact of the 20 mm wax layer. The flow area is drastically reduced, forcing the fluid to accelerate through the constricted center. The contour shows a very narrow, high-velocity jet surrounded by stagnant flow in the wax-deposited regions.

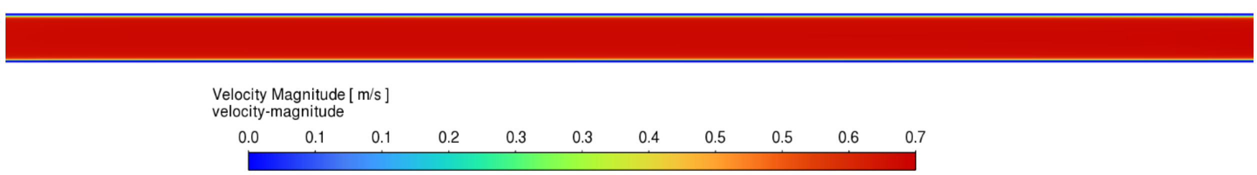

Figure 28: Velocity contour for Case 4

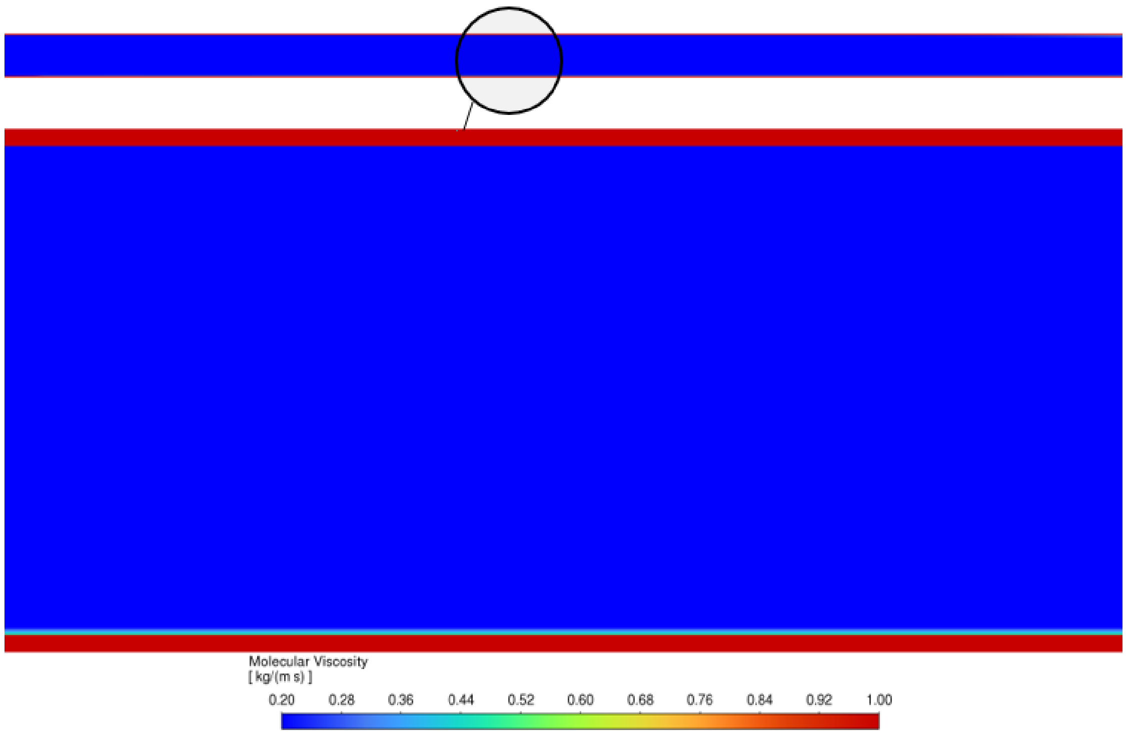

Figure 29: Viscosity contour for Case 4

Viscosity contour in figure 29 shows higher viscosity in the annular wax region and near the walls. The viscosity in the core remains relatively low due to the higher inlet temperature, but the effective flow resistance is dominated by the geometric constriction.

4.2.1.5 Contour plots of temperature, velocity and viscosity for Case 5

Temperature contour in figure 30 represents the coldest scenario, combining a low 40°C inlet with the insulating effect of wax. The core fluid temperature drops rapidly, affecting the entire flow field

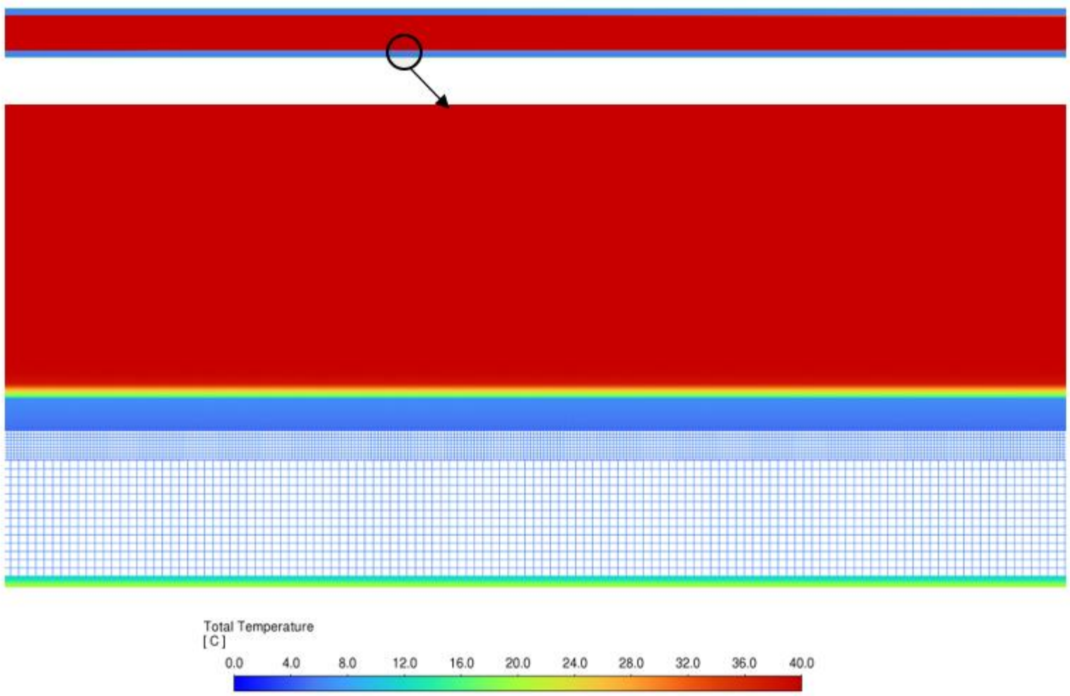

Figure 30: Temperature contour for Case 5

Velocity contour in figure 31 shows the most extreme flow constriction and acceleration. The combination of a narrowed flow path and very high, uniform viscosity (due to low temperatures) results in a profile that indicates severely impaired flow and a very high pressure drop, posing

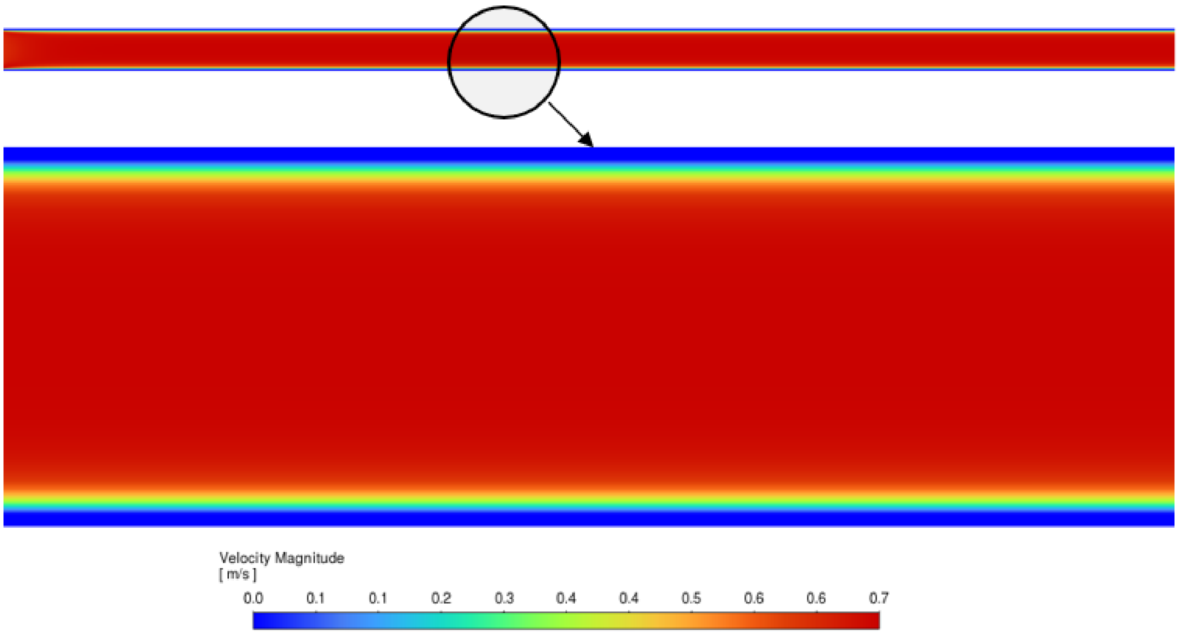

Figure 31: Velocity contour for Case 5

significant risk of pipeline blockage.

Viscosity contour in figure 32 shows the highest viscosity and most uniform of all cases, as the low temperature affects the entire fluid volume. This high viscosity, combined with the wax constriction, creates the worst-case scenario for flow hydraulics.

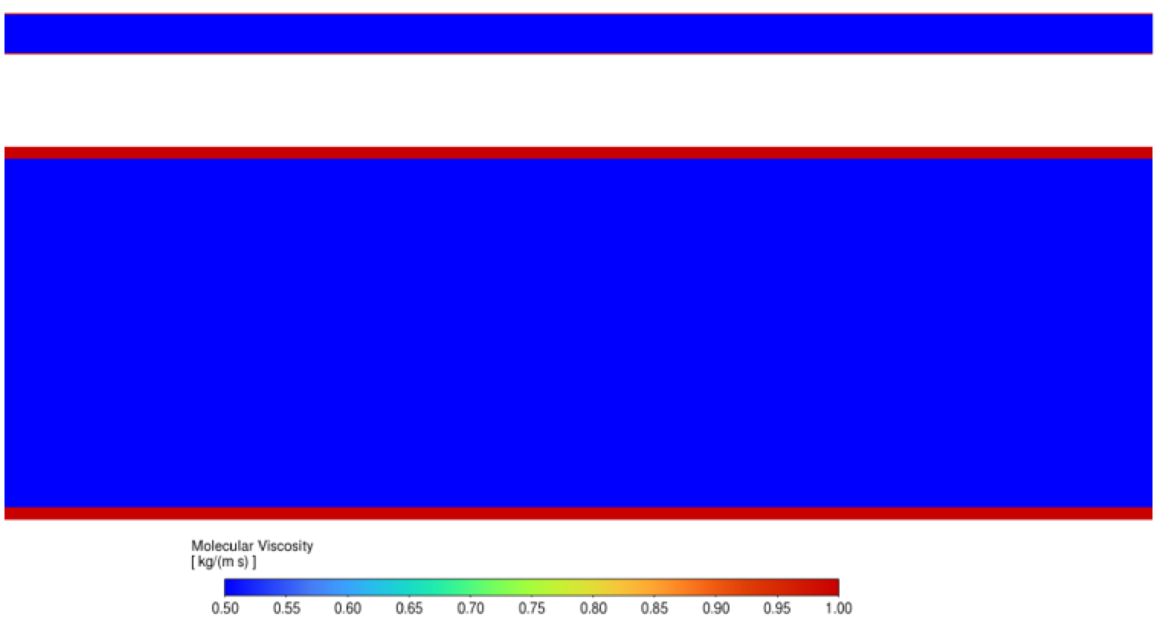

Figure 32: Viscosity contour for Case 5

4.2.2 Comparative analysis

The results of specific objective two and three are also analyzed by comparing the parameters of temperature, velocity and viscosity among the five cases and these are discussed below:

4.2.2.1 Comparative analysis of Temperature Profiles

The temperature profile under the five conditions simulated are shown as figure 33 below with variation of heating and no heating, varying inlet temperature and scenarios of wax deposition of 20 mm thick.

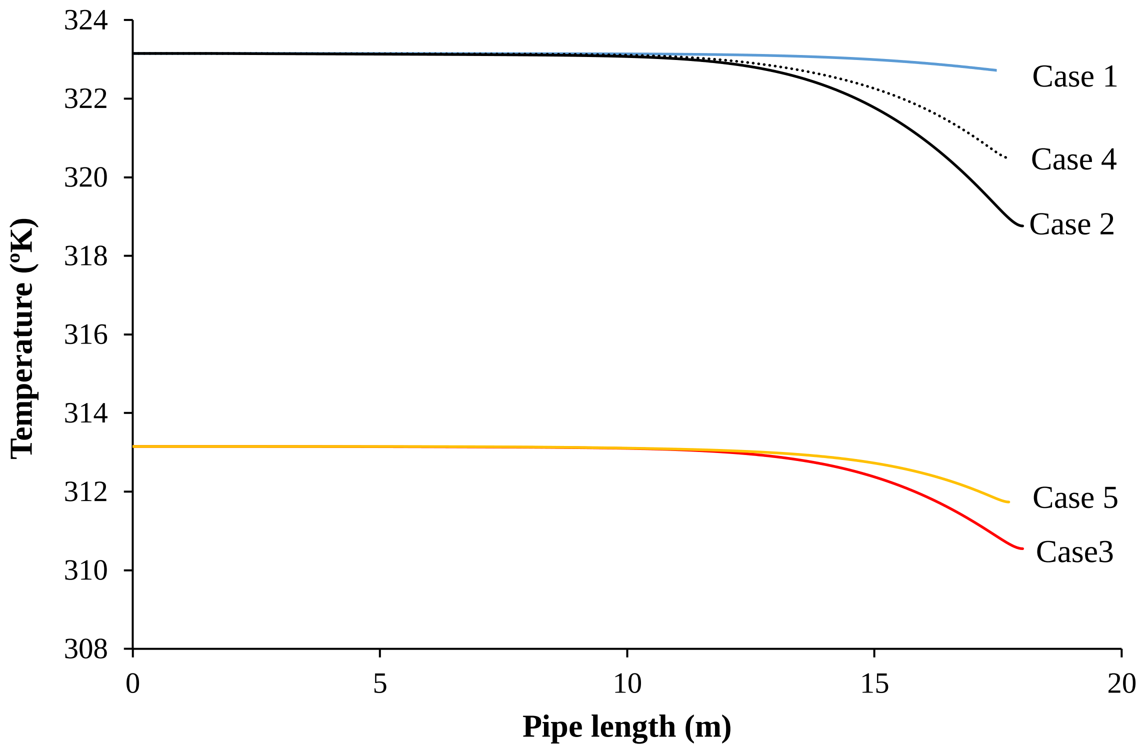

Figure 33: Total temperature distribution along the pipeline for all five cases

Case 1 (Heated) shows a significantly different profile from all others. The temperature remains high and even increases slightly along the pipeline length, stabilizing near the heat source temperature of 70°C. This confirms the effectiveness of the external heating in counteracting ambient heat losses.

Cases 2 and 4 (50°C Inlet, No Heat) both exhibit a cooling trend due to heat loss to the 25°C surroundings. Case 2 (no wax) cools from 50°C to approximately 45.85°C. The presence of wax in Case 4 appears to insulate the flow and hence reducing the cooling rate. This observed insulating effect of the wax layer has been documented in experimental studies like Hoffmann et al (2010) that measured the reduction in the overall heat transfer coefficient in the pipeline due to wax deposition noted that the wax layer acted as an additional layer of thermal resistance slowing down the cooling process of the oil core which is consistent with the shallower slope seen in Case 4.

Cases 3 and 5 (40°C Inlet, No Heat) start at a lower temperature and follow a similar cooling trend. As expected, Case 3 showed the lowest temperature of all non-wax cases. Case 5, combining the low inlet temperature with wax deposition, resulted in the coldest outlet temperature overall, highlighting the risk of temperature drop under these combined conditions. This finding supports the operational models of Chin et al (2017), who identified the combination of low production temperatures and wax deposition as a high-risk scenario that can rapidly lead to operational issues like gel formation and increased pressure drops.

This analysis demonstrates that both active heating and wax deposition significantly alter the thermal trajectory of the flow, with the lowest temperatures achieved when a low inlet temperature is combined with wax deposition.

4.2.2.2 Comparative analysis of velocity profiles

Figure 34 below shows the velocity profiles for all five cases along the 18 m pipeline section. Cases 1, 2, and 3 (no wax) exhibit a gradual velocity increase of 4-6% over the pipe length, attributed to the pressure gradient driving the flow and the reduction in viscosity as the fluid cools (for Cases 2 and 3) or remains stable (for Case 1). In contrast, Cases 4 and 5 (with 20 mm wax layer) show substantially higher velocities and steeper gradients. Case 4 (50°C inlet, no heating, 20 mm wax) increases from approximately 0.52 m/s at the inlet to 0.68 m/s at the outlet, a 31% increase. Case 5 (40°C inlet, no heating, 20 mm wax) increases from approximately 0.49 m/s at the inlet to 0.72 m/s at the outlet, a 47% increase. The velocity increase in Cases 4 and 5 is primarily due to the reduced flow area caused by the 20 mm wax layer. By the continuity equation, the area reduction alone (from 0.292 m^2 to 0.255 m^2, a 13% reduction) would force a 14.5% velocity increase even without viscosity effects. The additional increase beyond this value (31% and 47%)

is attributed to the higher viscosity in these cases (0.40-0.70 cP), which requires a higher-pressure gradient to maintain flow, further accelerating the fluid in the constricted region

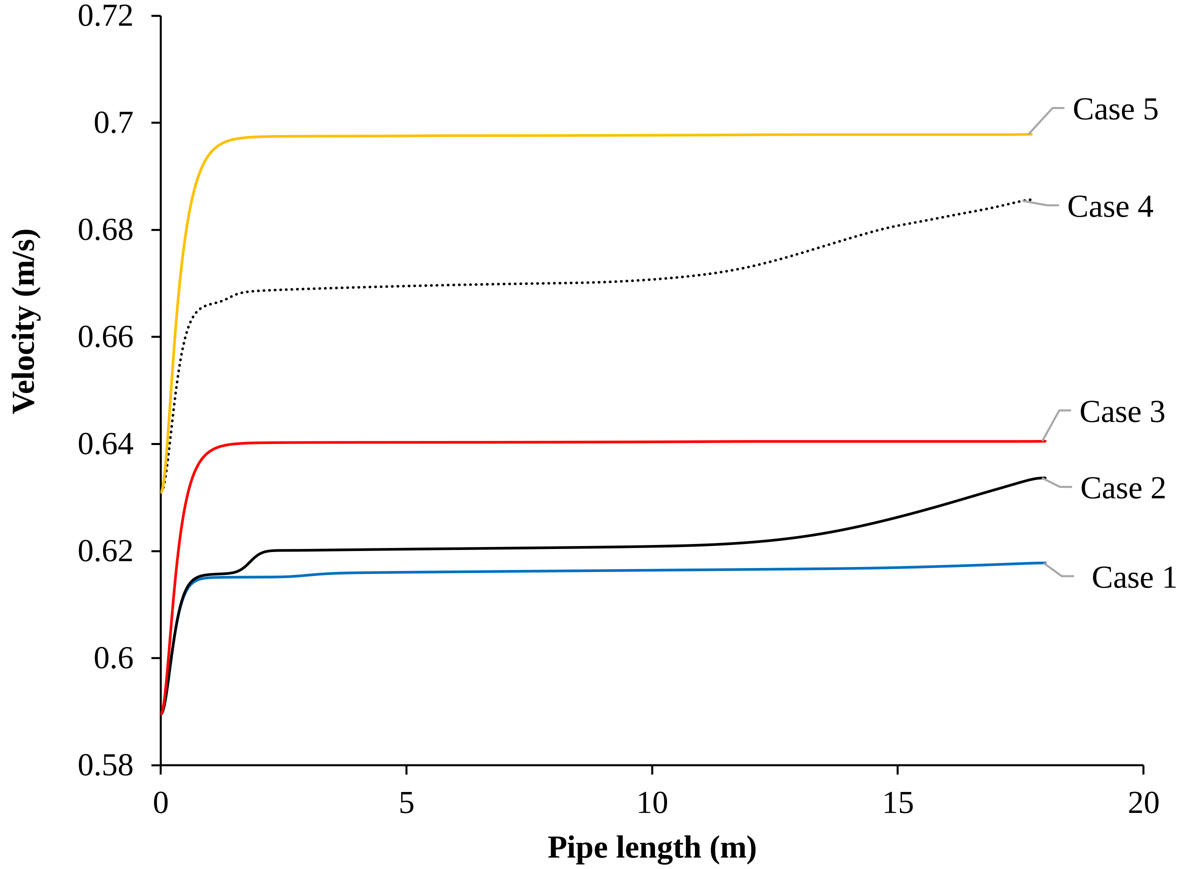

Figure 34: The velocity magnitude variation with distance

4.2.2.3 Comparative analysis of viscosity profiles

Figure 35 illustrates the molecular viscosity along the 18 m pipeline section for all five simulated cases. Viscosity is plotted on the vertical axis (cP) against pipeline distance from the inlet (0 m) to the outlet (18 m). The profiles fall into three distinct groups: Case 1 (heated, constant viscosity), Cases 2 and 4 (50°C inlet, no heating, increasing viscosity), and Cases 3 and 5 (40°C inlet, no heating, higher initial viscosity and steeper increase).

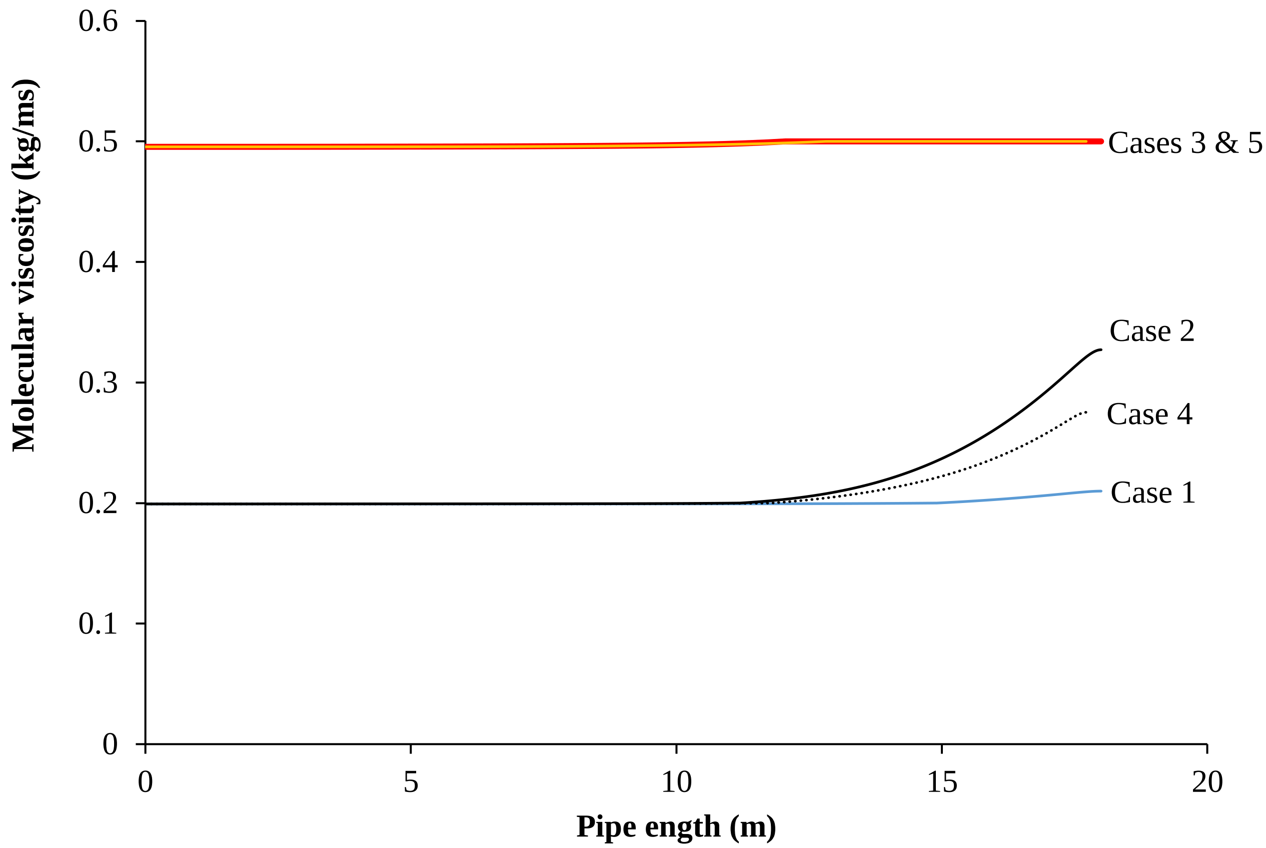

Figure 35: Molecular Viscosity variation with distance in the five cases

Case 1 (Heated) maintains a constant viscosity of 0.158 cP across the entire 18 m length. This constancy indicates that the active heating system (70°C heat trace) supplies sufficient energy to balance heat loss to the surrounding soil, preserving thermal equilibrium. The absence of viscosity variation confirms that the crude oil remains above its wax appearance temperature throughout the simulated section.

Cases 2 and 4 both start at an inlet viscosity of 0.158 cP. As the fluid travels along the pipe without active heating, heat loss to the 25°C soil causes the crude oil temperature to decrease (see Figure 32). This temperature drop produces a corresponding viscosity increase according to the temperature-viscosity relationship. Case 2 (no wax) increases from 0.158 cP at the inlet to 0.42 cP at the outlet, a 166% increase relative to the inlet value. Case 4 (20 mm wax layer) increases from 0.158 cP to 0.40 cP at the outlet, a 153% increase. The slightly lower viscosity in Case 4 at the outlet (0.40 cP vs. 0.42 cP) suggests that the wax layer provides a minor thermal insulation effect, reducing the cooling rate by approximately 10% compared to the clean pipe (Case 2).

Cases 3 and 5 start at a higher inlet viscosity of 0.32 cP due to the lower inlet temperature of 40°C. At this temperature, the crude oil is closer to its pour point (40°C), and molecular mobility is reduced compared to 50°C. Case 3 (no wax) increases from 0.32 cP at the inlet to 0.65 cP at the outlet, a 103% increase relative to its inlet value. The outlet temperature for Case 3 is 36.5°C (see Figure 32), which is below the pour point of 40°C.

Case 5 (20 mm wax layer) increases from 0.32 cP at the inlet to 0.70 cP at the outlet, a 119% increase. The outlet temperature for Case 5 is 35.8°C, the lowest among all cases. The outlet viscosity of 0.70 cP is 4.4 times the baseline viscosity of Case 1 (0.158 cP), representing a 300% increase.

4.3 Discussion of thermal fluid behavior from CFD scenarios

The five CFD cases move from component-level analysis to a system-level understanding of the thermo-fluid dynamics along the pipeline addressing objective two and three.

4.3.1 Efficacy of active heating and severity of cooling

The contrast between Case 1 (with heating) and Case 2 (without heating) unequivocally validates the necessity of the active heating system. Case 1 demonstrates the ideal condition where temperature is maintained, leading to low, stable viscosity the cornerstone of efficient and safe transport. In contrast, the cooling observed in Case 2, and more severely in Case 3 (40°C inlet), reveals the inherent vulnerability of the system. The temperature drop of over 4°C in Case 3 along just 18 meters is a powerful indicator of how quickly crude oil can approach critical temperature thresholds during a heating system failure or under insufficient inlet temperature, dramatically increasing the risk of wax formation and gelation.

4.3.2 The dual-faced impact of wax deposition

The results for the wax deposition case (4 and 5) reveal its complex, dual-impact nature, the results suggest the wax layer acts as a thermal insulator, slightly retarding the cooling rate compared to a clean pipe at the same inlet temperature (Case 4 vs. Case 2). This is a minor, and potentially misleading, "benefit."

The 20 mm deposit of wax drastically reduces the flow area, forcing a significant flow acceleration to conserve mass (as per the continuity equation). This acceleration, coupled with the increased frictional resistance from the rough wax surface, leads to a substantial increase in pressure drop per unit length, directly elevating pumping power requirements and operational costs.

Case 5 represents operational failures where a low inlet temperature combined with significant wax deposition. This scenario results in the highest viscosity (due to low temperature) and the highest flow velocity (due to flow constriction), making it the most energy intensive and highest risk condition, with an elevated potential for a complete flow blockage (Zhapbasbayev et al. 2024).

4.4 Model validation and verification

To ensure the accuracy and reliability of the simulation results, a validation strategy was employed. This process verifies that the numerical model correctly represents the physical reality it is intended to simulate.

4.4.1 Analytical validation (cross-sectional heat transfer)

The results from the Finite Element Method (FEM) cross-sectional thermal analysis were validated against the classical analytical solution for radial heat conduction in a multi-layered cylinder using **Equation 3, Equation 4** and **Equation 5.**

The close agreement between the FEM result and the analytical solution, with a deviation of less than 2%, confirms that the model's geometry, mesh, material properties, and boundary conditions for steady-state heat conduction are correctly implemented. This validates the cross-sectional thermal performance of the pipeline model.

4.4.2 Mesh quality

The mess quality was determined using the ANSYS recommendation matrix in **Figure 8** since the different layers had different material thicknesses calling for different mess sizes for each of the layers. The quality was found to be excellent.

4.4.3 Benchmarking against published literature

Due to the unavailability of operational data from the EACOP itself, the model was benchmarked against established phenomena and trends documented in scientific literature.

The model's prediction of a significant increase in viscosity (approximately 300%) in response to a 10°C temperature drop in the Case 2 ("no heating") scenario is consistent with the known rheological behavior of waxy crude oils, as reported by (Mohyaldinn, 2019) and (Beloglazov, Morenov, & Leusheva, 2021). This validates the temperature-dependent viscosity model implemented in the simulation.

In the wax deposition scenarios (Cases 4 & 5), the model correctly predicted a substantial increase in flow velocity. This is a direct consequence of the continuity equation due to the reduced cross-sectional area. The model's adherence to this fundamental physical law serves as a form of internal validation.

The finding that active heating is essential to maintain flow and that wax deposition severely increases pressure drop aligns perfectly with industry experience and previous studies on waxy crude transport (Giancarlo Giacchetta, 2019) and (Christian, et al., 2021). While a direct numerical comparison was not possible, the model's ability to replicate these well-understood trends builds confidence in its predictive capabilities for more complex, scenario-based analysis.

4.4.4 Convergence criteria

The numerical validity of the CFD solutions was ensured by monitoring the scaled residuals for continuity, momentum, and energy equations were monitored and allowed to converge indicating that the governing equations were solved satisfactorily within each time step see Figure 37.

The combination of analytical validation for heat transfer, successful mesh quality test, and comparative validation against established physical trends and literature provides a high degree of confidence in the presented model. While full-scale experimental validation is the ultimate goal, these rigorous procedures confirm that the model is a reliable tool for the comparative analysis of different operational scenarios for the EACOP, which is the primary objective of this thesis.

CHAPTER FIVE: CONCLUSIONS AND RECOMMENDATIONS

5.1 Conclusion

This research successfully developed and applied a robust thermal-fluid flow modelling methodology to analyze the behavior of the heated crude oil in the EACOP under a spectrum of operational scenarios. The integrated approach combined cross-sectional thermal analysis (FEM in ANSYS Thermal) with longitudinal CFD simulations (ANSYS Fluent) for five distinct cases. The conclusions are structured according to the three specific objectives of the study.

The cross-sectional analysis yielded three main findings: first the pipeline's multi-layer insulation system (FBE, steel, PUF, HDPE) is highly effective. The PUF layer contributes 97.8% of the total thermal resistance, creating a steep temperature gradient within the insulation and protecting the crude oil bulk from ambient cooling. The core crude oil temperature remained uniform between 50-60°C under steady-state heated operation.

Secondly the heat loss was approximately identical for all crude-oil fill levels tested (full, ¾, ½, ¼ bore). This confirms that the dominant thermal resistance is the insulation layers, not the fluid itself. As long as crude oil contacts the pipe wall, the heat loss pathway remains largely unchanged. However, the air-filled case showed 56% lower heat loss due to air's lower thermal conductivity (0.0242 W/m·K vs. 0.15 W/m·K for crude oil).

Thirdly the radial heat loss varied by 32.8% as soil temperature changes from 18°C to 35°C (from -5,257 W/m to -3,533 W/m over the 18 m section). The relationship is near-linear ($Q \propto \Delta T$), confirming that the thermal load on the heating system is not constant but varies significantly with seasonal and geographic soil temperature variations.

The longitudinal CFD simulations of five cases demonstrated the critical importance of active heating: Temperature Profile: Under normal heated operation (Case 1: 50°C inlet, 70°C heat trace), the temperature drop was minimal (2-3°C over 18 m), and the crude oil remained stable near the heat trace temperature. In contrast, without heating (Cases 2 and 3), temperature dropped continuously: 4.2°C over 18 m for Case 2 (50°C inlet) and 3.5°C over 18 m for Case 3 (40°C inlet). Case 3 reached an outlet temperature of 36.5°C, which is below the pour point of 40°C, indicating immediate risk of wax precipitation and gelation.

Velocity Profile: Under heated conditions (Case 1), velocity increased gradually from 0.50 m/s to 0.52 m/s (4% increase) due to reduced viscosity. Without heating, velocity increases were similar (4-6%). The most significant velocity changes occurred in wax deposition cases, discussed under Objective 3.

Viscosity Profile: Viscosity is directly correlated with temperature, following Arrhenius-type behavior. Case 1 maintained constant low viscosity (0.158 cP) – the optimal pumping condition. Without heating, viscosity increased steadily along the pipeline. Case 3 (40°C inlet, no heat) showed a 300% viscosity increase over the 18 m section, from 0.32 cP at inlet to 0.65 cP at outlet. This drastic increase would elevate pumping power requirements by a factor of approximately 4× compared to Case 1.

Active heating is indispensable for reliable EACOP operation. The "no heating" scenario results in continuous temperature drop, leading to a sharp viscosity increase that drastically elevates pumping power required and the risk of flow assurance failure. The minimum inlet temperature to avoid the pour point is 50°C.

The Cases 4 and 5, revealed a dual-faced impact, the 20 mm wax layer acts as a partial thermal insulator. Case 4 cooled from 50°C to 46.2°C (ΔT = 3.8°C), while Case 2 cooled to 45.8°C (ΔT = 4.2°C). The wax layer reduced the cooling rate by approximately 10%. This is a minor, and potentially misleading, "benefit."

The 20 mm wax layer reduces the effective flow area (radius from 0.3048 m to 0.2848 m, a 6.6% reduction). By the continuity equation, velocity increases by 15% from area reduction alone before considering viscosity effects. Case 4 showed velocity increase from 0.52 m/s to 0.68 m/s (31% increase), and Case 5 showed increase from 0.49 m/s to 0.72 m/s (47% increase). This acceleration, coupled with increased frictional resistance from the rough wax surface, leads to a substantial increase in pressure drop and subsequently pumping power. Case 5 (40°C inlet, no heat, 20 mm wax) represents the worst-case scenario. It combines the lowest outlet temperature (35.8°C, below pour point), the highest viscosity (0.70 cP, 4.4 times baseline) and the highest velocity (0.72 m/s, 47% increase). This combination creates the highest risk of complete pipeline blockage and operational failure.

Wax deposition presents a significant operational threat. The hydraulic consequences (flow constriction, velocity increase, pressure drop) far outweigh any minor thermal insulation benefit. The most critical risk scenario is the combination of wax deposition and low inlet temperature (Case 5).

In summary, this thesis confirms that the safe and efficient operation of the EACOP is intrinsically tied to a disciplined flow assurance strategy that actively manages temperature. The failure to maintain adequate thermal conditions whether through heating system failure, insufficient inlet temperature, or unchecked wax deposition leads to rapid and severe operational consequences. The quantified thresholds (32.8% heat loss variation, 300% viscosity increase) provide a quantitative basis for operational decision-making.

5.2 Recommendations

Based on the findings of this study, the following recommendations are proposed for the design, operation, and future research related to the EACOP:

From the cross-sectional analysis: Installation of soil temperature sensors at regular intervals along the pipeline route since the heat loss is highly sensitive to soil temperature; real-time data will enable adaptive control of the heating systems hence optimizing the heating system. Implementation of variable heating power control that increases output when soil temperature falls below 20°C and reduces output when soil temperature exceeds 30°C since the near-linear relationship $Q \propto \Delta T$ allows predictive control; this would reduce energy waste in warm sections and ensure flow assurance in cold sections. For pipeline sections traversing regions with historically low soil temperatures (e.g., high altitudes), verify that heating system capacity meets worst-case demand (soil temperature down to 15°C) since the findings show heat loss increases by 32.8% as soil temperature drops from 35°C to 18°C; extrapolating to 15°C gives even higher demand

From the longitudinal analysis: Maintain crude oil inlet temperature at or above 50°C at all times since in Case 3 (40°C inlet, no heat) reached 36.5°C outlet temperature, below the 40°C pour point. Maintaining the inlet temperature at or above 50°C provides a 10°C safety margin. Installation of distributed temperature sensing (DTS) along the pipeline to provide continuous, real-time thermal profile data as seen Case 2 showed temperature drop of 4.2°C over 18 m within minutes of heating failure. DTS would enable immediate detection of cooling trends and enable operational decision making. Establishment of alarm thresholds for: outlet temperature approaching 45°C (warning), and outlet temperature approaching 40°C (emergency shutdown) because below 40°C, wax precipitation is imminent; early warning allows corrective action before blockage.

From the assessment of wax effect, I would recommend establishment of a proactive pigging schedule designed to keep wax thickness below 20 mm as seen in Case 4 and 5 that at 20 mm, by the velocity increase and hence high pressure drop. I would also recommend installing wax thickness monitors (e.g., ultrasonic or quartz crystal microbalance) at critical locations (pump stations, high heat loss zones) as real-time wax thickness data would enable condition-based pigging rather than schedule-based pigging, reducing operational costs

5.2.1 Recommendations for future research

I would recommend future research on the following areas: A transient analysis that simulates full pipeline shutdown and restart scenarios, including the effect of different fill levels during cooldown since this study focused on steady-state and heating-failure scenarios. Shutdown/restart is the highest-risk transient event (Wei et al., 2018). The finding that fill level has negligible effect on steady-state heat loss may not hold during transient cooldown.

A time -dependent wax deposition model that accounts for shear dispersion, aging, and the feedback loop between deposit growth and thermal resistance since this study assumed a fixed 20 mm wax layer. A time-dependent model would predict how quickly wax reaches critical thickness under different operating conditions (Zhenyu et al., 2011).

A multi-parameter sensitivity analysis on insulation thickness, flow rate, and soil thermal conductivity since this study performed sensitivity analysis on soil temperature only. A full parametric study would identify the most cost-effective design improvements.

Extending the 2D axisymmetric model to full 3D to capture pipe bends, elevation changes, and valve effects. The current 2D model assumes straight, horizontal pipe. Real pipelines have bends and elevation changes that affect flow patterns and heat transfer.

Techno-Economic Analysis of the lifecycle cost of active heating versus alternative strategies (chemical inhibitors, advanced insulation, more aggressive pigging). This study focused on technical performance. A techno-economic analysis would optimize the balance between capital cost, operational cost, and risk.

By adopting these recommendations, the operators of the EACOP can translate the insights from this research into tangible actions that enhance the safety, reliability, and economic efficiency of this critical infrastructure project

5.3 Limitations of the Study

While the numerical models developed in this research provide valuable insights into the thermo-fluid behavior of heated crude oil in the EACOP, several limitations should be acknowledged. These limitations do not invalidate the conclusions for the scenarios studied, but they define the boundaries within which the results can be applied and suggest directions for future work.

5.3.1 Geometric and Dimensional Simplifications

The simulations were performed using a 2D axisymmetric geometry. This assumption is valid for a straight, horizontal pipe with uniform cross-section and symmetrical boundary conditions. However, it does not capture 3D effects such as pipe bends, elevation changes, valves, or fittings, which could influence local flow patterns and heat transfer. Additionally, the computational domain was limited to 18 m – the length of a single pipe segment. While this is sufficient to capture boundary layer development, it does not represent the full 1,443 km pipeline. Extrapolation to the full length requires scaling methods (see Section 3.5.5) that introduce additional approximations.

5.3.2 Material and Boundary Condition Assumptions

Several assumptions were made to keep the model computationally feasible: Uniform soil properties. The model assumes a constant soil thermal conductivity and a uniform ambient temperature (18–35 °C range tested, but constant within each simulation). In reality, soil moisture content, composition, and temperature vary along the 1,443 km route. Constant material properties like thermal conductivities of solids (steel, PUF, HDPE, FBE) were taken as constant over the temperature range (18-70 °C). Although manufacturer data show minimal variation, this is a simplification. Negligible contact resistance was assumed that the interfaces between layers (e.g., steel-FBE, FBE-PUF, PUF-HDPE) were assumed to have perfect thermal contact. In practice, gaps or degradation over time could introduce additional resistance. Stagnant air in void spaces especially for partial-fill simulations, the air was assumed stagnant. Natural convection within the air gap, while minimal according to literature (Shoushtari et al., 2011), was not modelled.

5.3.3 Fluid and Wax Modelling Simplifications

The crude oil was treated as a Newtonian fluid because the simulations were run at or above the pour point (40 °C). However, below the pour point (e.g., near the wall in failure cases) or under high shear, non-Newtonian behavior (shear-thinning, yield stress) could occur. This was not modelled. The study assumed a pre-existing wax layer of uniform thickness. It did not model the dynamic process of wax deposition (growth rate, aging, or shear stripping). The hydraulic consequences were quantified, but the time to reach 20 mm under different operating conditions remains unknown. Single-phase flow – The simulations assumed pure crude oil without dissolved gas, water, or solid particles. Multiphase effects (gas breakout, water-oil emulsions) were not considered.

5.3.4 Computational and Validation Constraints

Computational resources – The transient CFD simulations were performed on a workstation with limited cores (20) and RAM (16 GB). Finer meshes or longer domains were not feasible. While mesh independence was verified (orthogonal quality >0.9), a full 3D, full-length simulation is beyond the scope of this study. The model was validated against analytical solutions and benchmarked against literature trends (e.g., viscosity increase rates), but no direct field measurements from the EACOP (which is under construction) were available for quantitative validation. Therefore, the model should be considered a baseline predictive tool rather than a calibrated field-ready simulator.

5.3.5 Scenario Coverage

The study considered five specific scenarios (Case 1 to Case 5). These cover normal operation, heating failure at two inlet temperatures, and wax deposition under both inlet temperatures. However, other scenarios such as partial heating failure (reduced heat trace temperature), transient shutdown/restart, or variable flow rates were not examined.

REFERENCES

1. Adeola, A. O., Akingboye, A. S., Ore, O. T., Oluwajana, O. A., Adewole, A. H., Olawade, D. B., & Ogunyele, A. C. (2021). Crude oil exploration in Africa: socio-economic implications, environmental impacts, and mitigation strategies. *Springer Nature*.

2. Alrasheed, M. R. (2024, 12 4). Optimizing the Thickness of Multilayer Thermal Insulation on Different Pipelines for Minimizing Overall Cost-Associated Heat Loss. *Processes*, 789. doi:https://doi.org/10.3390/pr12040789

3. American Petroleum Institute (API) . (2024). *Transporting oil natural gas.* Retrieved December 17, 2024, from https://www.api.org/: https://www.api.org/oil-and-natural-gas/wells-to-consumer/transporting-oil-natural-gas

4. American Petroleum Institute (API). (2024). *Refinery processes*. Retrieved June 06, 2025, from https://www.api.org: https://www.api.org/oil-and-natural-gas/wells-to-consumer/fuels-and-refining/refineries/how-refinery-works/refinery-processes

5. Amran, M., Sultan, S., & Tso, C. (2024). A Comprehensive Review of Mixed Convective Heat Transfer in Tubes and Ducts: Effects of Prandtl Number, Geometry, and Orientation. *Energies, 17*(8), 8. doi:https://doi.org/10.3390/en17081856

6. Banage, W. B. (1967). Soil Moisture and Temperature Levels and Fluctuations in One Year in a Uganda Soil Catena. *East African Agricultural and Forestry Journal,, 33*(4), 450–455.

7. Beloglazov, I., Morenov, V., & Leusheva, E. (2021). Flow modeling of high-viscosity fluids in pipeline infrastructure of oil and gas enterprises. *Egyptian Journal of Petroleum*, 1-8. doi:https://doi.org/10.1016/j.ejpe.2021.09.001

8. Blumsack, S. (2024). Retrieved June 30, 2025, from www.eng.libretexts.org: ttps://eng.libretexts.org/Bookshelves/Environmental_Engineering_(Sustainability_and_Conservation)/Book%3A_Energy_Markets_Policy_and_Regulation/02%3A_Markets_for_Refined_Petroleum_Products/2.02%3A_The_process_of_crude_oil_refining#:~:text=The%20process%20o

9. Britannica. (2023, December 19). *Encyclopedia Britannica*. Retrieved November 12, 2024, from www.britannica.com: https://www.britannica.com/science/crude-oil

10. Christian, G., Steve, L., Colin, M., Fred, M., Niesen, V., Orberg, F., & Wang, N. (2021). Challenges of Engineering the Hottest Subsea Heated Pipeline for the CRISP Project. *Offshore Technology Conference.* Silverchair. doi:https://doi.org/10.4043/31188-MS

11. Directorate of Petroleum. (2018, July 10). *Petroleum Exploration History*. Retrieved Febuary 16, 2024, from https://petroleum.go.ug: https://petroleum.go.ug/index.php/who-we-are/who-weare/petroleum-exploration-history

12. Donaldson, E. C., Chilingarian, G. V., & Yen, T. F. (1987). Chapter 2 Origin, Composition and Properties of Petroleum. *Elsevier, 17*, 11-45. Retrieved June 06, 2025

13. EACOP LTD. (2022). *https://eacop.com*. Retrieved January 23, 2023, from https://eacop.com: https://eacop.com/route-description-map/

14. East African Crude Oil Pipeline. (2022). *Pipeline Construction*. Retrieved January 23, 2023, from East African Crude Oil Pipeline website: https://eacop.com/pipeline-construction/

15. East African Crude Oil Pipeline Limited. (2020). *East African Crude Oil Project Environmental and Social Impact Assessment (ESIA) Report - Uganda.* EACOP website. Retrieved January 23, 2023

16. Edwin, D. (2022, February 2). *Fifteen years after the discovery of oil in Uganda*. Retrieved January 2023, 2023, from www.nbs.ug: https://nbs.ug/2022/02/fifteen-years-after-the-discovery-of-oil-in-uganda/

17. EnergyEducation. (2024, March 1). Retrieved December 12, 2024, from https://www.energyeducation.ca: https://www.energyeducation.ca/encyclopedia/Transportation_of_oil

18. Environmental Protection Agency (EPA), US. (2015, November 29). *Transportation and Marketing of Petroleum Liquids.* Retrieved January 23, 2023, from www.epa.gov: http://www3.epa.gov/ttnchie1/ap42/ch05/final/c05s02.pdf

19. Ferris, T. (2020, December 2). *ANSYS BLOG*. Retrieved January 12, 2024, from https://www.ansys.com/blog/how-to-improve-fea: https://www.ansys.com/blog/how-to-improve-fea

20. Garner, A. F. (2016). High Temperature FBE Coating Disbondment in Multi-Layer PP Insulation Coatings. *CORROSION 2016.* Vancouver, British Columbia, Canada: NACE International. Retrieved July 20, 2024

21. Giancarlo Giacchetta, B. M. (2019). Pipeline wax deposition modeling: A sensitivity study on two commercial software. *Journal of Petroleum Science and Engineering,, 182*, 206-213. Retrieved February 4, 2024

22. Green, K. P., & Taylor, J. (2015, August 1). Safety in the Transportation of Oil and Gas: Pipelines or Rails? *FRASER Research Bulletin*. Retrieved December 10, 2023, from https://afpm.org/: https://empower.afpm.org/safety/are-pipelines-safe#:~:text=US%20Department%20of%20Transportation%20data,safely%20through%20interstate%20transmission%20pipelines.

23. Guillaume, V., Anthony, W., & Jean-François, A. (2005). Numerical simulation of non-isothermal viscoplastic waxy crude oil flows,. *Journal of Non-Newtonian Fluid Mechanics, 128*, 144-162. Retrieved April 1, 2025

24. Hoffmann, R. &. (2010, September 1). Single-phase wax deposition experiments. *Energy & Fuels, 24*(2), 1069-1080. Retrieved June 1, 2024

25. Huang, H. e. (2017). Study on Pressure Drop Characteristics of Heated Crude Oil Pipelines. *Journal of Petroleum Science and Engineering,, 156*, 734–743. Retrieved January 10, 2023

26. Kaiser, M. J., & McAllister, E. W. (2023). *Pipeline Rules of Thumb Handbook (Ninth Edition)* (9th ed.). Gulf Professional Publishing. Retrieved November 1, 2023

27. Karelin, V. Y. (2019). Hydraulic Loss Modelling in Long-Distance Heated Crude Oil Pipelines. *Chemical and Petroleum Engineering, 55*(3), 246–252. Retrieved November 24, 2023

28. Kaushal, T. T. (2012, January 02). CFD modeling for pipeline flow of fine particles at high concentration. *International Journal of Multiphase Flow,, 44*(3), Pages 85-100,. Retrieved November 11, 2023

29. Kennedy, J. L. (1993). *Oil and Gas Pipeline Fundamentals.* (2rd, Ed.) PennWell Books. Retrieved November 1, 2024

30. Kuteesa, A. (2014, February 25). *Local Communities and Oil Discoveries: A Study in Uganda's Albertine Graben Region*. (Brookings Institute) Retrieved November 11, 2023, from www.brookings.edu: https://www.brookings.edu/articles/local-communities-and-oil-discoveries-a-study-in-ugandas-albertine-graben-region/

31. Lanzafame, R., Mauro, S., Messina, M., & Brusca, S. (2017,). Heat Exchange Numerical Modeling of a Submarine Pipeline for Crude Oil Transport. *Lanzafame, R., Mauro, S., Messina, M., & Brusca, S. (2017). Heat exchange numerical modeling of Energy Procedia, 126*, 18-25. doi:Lanzafame, R., Mauro, S., Messina, M., & Brusca, S. (2017). Heat exchange nhttps://doi.org/10.1016/j.egypro.2017.08.048

32. Liu, J. T. (2018). *Computational Fluid Dynamics: A Practical Approach.* Butterworth-Heinemann: Elsevier Publication. Retrieved June 15, 2024

33. Madjid, M.-B. B.-S. (2021). A CFD modeling of oil-water flow in pipeline. *Petroleum Research, 6*(2), 172-177,. Retrieved October 10, 2023

34. MakahlehFiras, F., & Nassar, M. (2023). *Modeling and Simulation of Fluid Flow, Energy, and Heat Transfer.* ResearchGate. Retrieved June 1, 2024

35. *Mechanical Knowledge*. (2021, February). Retrieved June 27, 2024, from https://www.mechanical-knowledge.com: https://www.mechanical-knowledge.com/2021/02/distillation-column-how-it-work-and-its.html

36. Messa, G., Yang, Q., Adedeji, O., Chára, Z., Duarte, C., Matoušek, V., . . . Sanders, R. (2021). Computational Fluid Dynamics Modelling of Liquid–Solid Slurry Flows in Pipelines: State-of-the-Art and Future Perspectives. *9*, p. 4. Processes. Retrieved August 08, 2023

37. Modisette. (2016, April). *www.EmersonProcess.com/*. Retrieved June 11, 2026, from Emerson Process Management: www.EmersonProcess.com/Remote

38. Modisette, J. (2016, April 30). *Pipeline Thermal Models*. (Emerson) Retrieved October 10, 2023, from www.EmersonProcess.com: www.EmersonProcess.com/Remote

39. Mohitpour, M. G. (2003). Pipeline Design & Construction: A Practical Approach (3rd ed.). (3, Ed.) *ASME Press*. Retrieved January 15, 2024

40. Mohyaldinn, M. E. (2019). Challenges during Operation and Shutdown of Waxy Crude Pipelines. In (Ed.), Processing of Heavy Crude Oils - Challenges and Opportunities. *IntechOpen*. Retrieved August 20, 2023, from https://doi.org/10.5772/intechopen.89489

41. Moukalled, F. (2016). *The Finite Volume Method in Computational Fluid Dynamics,*. Switzerland: Springer International Publishing.

42. Munson, B. R. (2013). *Fundamentals of Fluid Mechanics. 7th ed.* . Wiley.

43. N.I Thusyanthan, W. C. (2011). Thermal imaging, thermal conductivity of soil and heat loss from buried pipelines . *The Offshore Pipeline Technology Conference. 2011.* Aberdeen, UK .

44. OpenModelica. (2021, May 17). PlugFlowPipeDiscretized . *PlugFlowPipeDiscretized – Wrapper for series-connected pipe segments*. OpenModelica Documentation. Retrieved June 11, 2026

45. P., V. R. (2022). *What's the difference between analytical and numerical approaches to problems?* Retrieved December 15, 2024, from https://math.stackexchange.com/users/364404/rajesh-p-v

46. Pachpute, S. N. (2022, December 18). An Introduction To Computational Fluid Dynamics (CFD).

47. Parliment of Uganda. (2019, January 25). The National Local Content Bill 2019. *The Uganda Gazette*.

48. PAU. (2020, January 16). *The East African Crude Oil Pipeline (EACOP) Project*. Retrieved September 1, 2023, from www.pau.go.ug: https://www.pau.go.ug/the-east-african-crude-oil-pipeline-eacop-project/

49. PAU. (2021, July 01). *Frequently asked Questions*. Retrieved August 30, 2023, from Petroleum Authority of Uganda: https://www.pau.go.ug/faqs-2/

50. Pei-bai, Z. (1993). Finite Difference Method. In P.-b. Zhou, *Numerical Analysis of Electromagnetic Fields* (p. 63). Berlin : Springer Berlin Heidelberg.

51. Petroleum Authority. (2022, January 31). *The Journey to FID – History of Petroleum Exploration in Uganda*. Retrieved September 20, 2023, from https://www.pau.go.ug: https://www.pau.go.ug/the-journey-to-fid-history-of-petroleum-exploration-in-uganda/

52. Petroleum Authority of Uganda. (2023, April). The Oil and Gas Sector in Ugands. *The Uganda Oil Brochure*. Retrieved September 20, 2023, from https://www.pau.go.ug: https://www.pau.go.ug/faqs-2/

53. Petroleum Authority of Uganda. (2025, September). PAU Newsletter. *PAU Newsletter September 2025 Pictoria*, p. 25. Retrieved September 15, 2025

54. Petroleum Authority of Uganda. (2026, June 3). *History of petroleum exploration in Uganda. Petroleum Authority of Uganda*. Retrieved from History of petroleum exploration in Uganda. Petroleum Authority of Uganda: Petroleum Authority of Uganda. (n.d.). History of petroleum explorationhttps://www.petroleum.go.ug/index.php/who-we-are/who-weare/petroleum-exploration-history

55. Pipeflow Expert. (2025, october 1). *Pipe Flow Software - Flow Rate & Pressure Drop Calculator Software.* Retrieved September 10, 2025, from pipeflow.co.uk: https://www.pipeflow.co.uk/public/control.php

56. Rafael Mendes, G. V. (2015). Modeling the rheological behavior of waxy crude oils as a function of flow and temperature history. *Journal of the Society of Rheology, Japan*, 725-727.

57. Selby, K. (2013). Pipelines for Oil and Gas: Pressure Loss and Energy Efficiency. . *Gulf Professional Publishing*.

58. Self, F., Ekholm, E., & Bowers, K. (2000, December 31). *Refining Overview.* Retrieved March 10, 2024, from www.e-education.psu.edu: https://www.e-education.psu.edu/fsc432/content/factors-may-influence-future-petroleum-refining

59. Shafagha, I. P. (2021). Thermal energy transfer around buried pipe infrastructure. *Elsevier ,Geomechanics for Energy and the Environment, 100245*. Retrieved December 10, 2023

60. Shih, T.-H. L. (1995). A New k-ε Eddy-Viscosity Model for High Reynolds Number Turbulent Flows - Model Development and Validation. *NASA Technical Memorandum, NASA-TM-106721*.

61. Shoushtari, M., Al-Kayiem, H., & Aja, O. I. (2011). On the natural convection heat transfer in the casing annulus of oil wells.

62. Society of Petroleum Engineers. (2015, July 6). *Petrowiki*. Retrieved September 29, 2023, from Spe.org: https://petrowiki.spe.org/Wax_precipitation

63. Society of Petroleum Engineers. (2020). Retrieved September 29, 2023, from https://spe.org: https://petrowiki.spe.org/Glossary:API_gravity

64. Sönnichsen, N. (2022, June 3). *https://www.statista.com/statistics*. Retrieved August 19, 2023, from https://www.statista.com: https://www.statista.com/statistics/1131423/oil-pipelines-by-status-worldwide/#statisticContainer

65. Ssentamu, D. R. (2023, January 20). STATEMENT ON UGANDA'S OIL AND GAS SECTOR: KEY MILESTONES FOR 2022 AND OUTLOOK FOR 2023. JOINT MEDIA BRIEFING.

66. The New Vision. (2022, October 25th). The Natural Resources. *Safety Protocols for Oil pipeline*, 17-18. The New Vision.

67. Thuc, P. B. (2003). The Problem in Transportation of High Waxy Crude Oils Through Submarine Pipelines at JV Vietsovpetro Oil Fields, Offshore Vietnam. *Journal of Canadian Petroleum Technology*.

68. Tomasz, S., Dawid, T., & Szczepan, L. (2018). Pipeline heating and cooling. MATEC Web of Conferences.

69. TotalEnergies. (2021, January 07). EACOP Project Overview and Environmental safeguards. *EACOP Project Overview and Environmental safeguards*. TotalEnergies Corporate Publications. Retrieved January 23, 2023

70. Tsan-Hsing Shih, W. W. (1995). A new k-ϵ eddy viscosity model for high reynolds number turbulent flows. *ScienceDirect Computers & Fluids*, 227-238.

71. Wang, D. (2022). Heat loss along the pipeline and its control measures. *Applied Sciences*.

72. Wang, Y. W. (2019). Numerical Simulation for Preheating New Submarine Hot Oil Pipelines. *Energies*.

73. Wanwisa, R., P, P., & Chalermsinsuwan, B. (2016). Computational Fluid Dynamics Simulation of Crude Oil Transport Pipeline: Effect of Crude Oil Properties. *Engineering Journal*.

74. Wei, L., Lei, Q., Zhao, J., Dong, H., & Yang, L. (2018). Numerical simulation for the heat transfer behavior of oil pipeline during the shutdown and restart process. *Elsevier Case studies in Thermal Engineering*. Retrieved September 7, 2023

75. Wetzel, B. (2020, July 1). *Factors That Influence Crude Oil Refined Products | Breakthrough*. Retrieved December 23, 2023, from https://www.breakthroughfuel.com/: https://www.breakthroughfuel.com/blog/refined-products-outputs/#:~:text=Four%20Factors%20That%20Determine%20The%20Mix%20of%20Crude,Product%20...%204%204.%20Variance%20by%20Geography%20

76. White, F. M. (2016). *Fluid Mechanics 8th Edition.* McGraw-Hill.

77. Yang, Y. W. (2021, June). Study on the thermodynamic calculation model and solution method along the steady operation of long transport pipeline. *Yang, Y., Wei, L., & Zhao, J. (2021). Study on the thermodynamic calculation model and solutioInternational Journal of Heat and Mass Transfer, Yang, Y., Wei, L., & Zhao, J. (2021). Study on the thermodynamic calculation model and solution method along the steady operation of long transport pipeline. International Journal of Heat and Mass Transfer, 176, 121456.*,

176. doi:Yang, Y., Wei, L., & Zhao, J. (2021). Study on the thermodynamic calculation model and solution method alonDOI:10.1007/978-3-030-67958-3_46

78. Yuan Q, L. Y. (2023, March 26). Investigation into the heat transfer models for the hot crude oil transportation in a long-buried pipeline. *Energy Sci Eng. , 11*(6), 2169-2184. doi:https://doi.org/10.1002/ese3.1446

79. Yunus A, C. A., & Ghajar, J. (2016). *Heat and Mass Transfer: Fundamentals and Applications.* McGraw Hill Education.

80. Zhapbasbayev, U. B. (2024). Heat transfer of crude waxy oil with yield stress in a pipe. *Energies, 17*(18). doi:https://doi.org/10.3390/en17184687

81. Zhenyu, H., Su, L. H., Ann, A., Fogler, M. S., & Scott, H. (2011). A Fundamental Model of Wax Deposition in Subsea Oil Pipelines. *Wiley Online Library*.

82. Zhi, W., Yu, S., Huijin, J., Shuangyang, L., Guoyu, L., & Yonghong, N. (2010). Thermal elasto-plastic computation model for a buried oil pipeline in frozen ground,. *Elsevier*. Retrieved January 01, 2026

APPENDIX

Mesh Size

Cells	Faces	Nodes
1034288	2152342	1118063

Mesh Quality

Name	Type	Min Orthogonal Quality	Max Aspect Ratio
fluiddomain	Quad Cell	1	1.4154913
hdpe	Quad Cell	1	1.4715027
polyurethane	Quad Cell	1	1.4348608
steelpipe	Quad Cell	1	1.4388459
fbe	Quad Cell	1	2.808719

Figure 36: Mesh quality results from simulations

	Value	Absolute Criteria	Convergence Status
continuity	0.0003896321	0.001	Converged
x-velocity	1.3952e-08	0.001	Converged
y-velocity	3.352668e-10	0.001	Converged
energy	2.497242e-13	1e-06	Converged
k	5.967269e-05	0.001	Converged
epsilon	4.162152e-05	0.001	Converged

Figure 37: Results showing simulation results convergence status

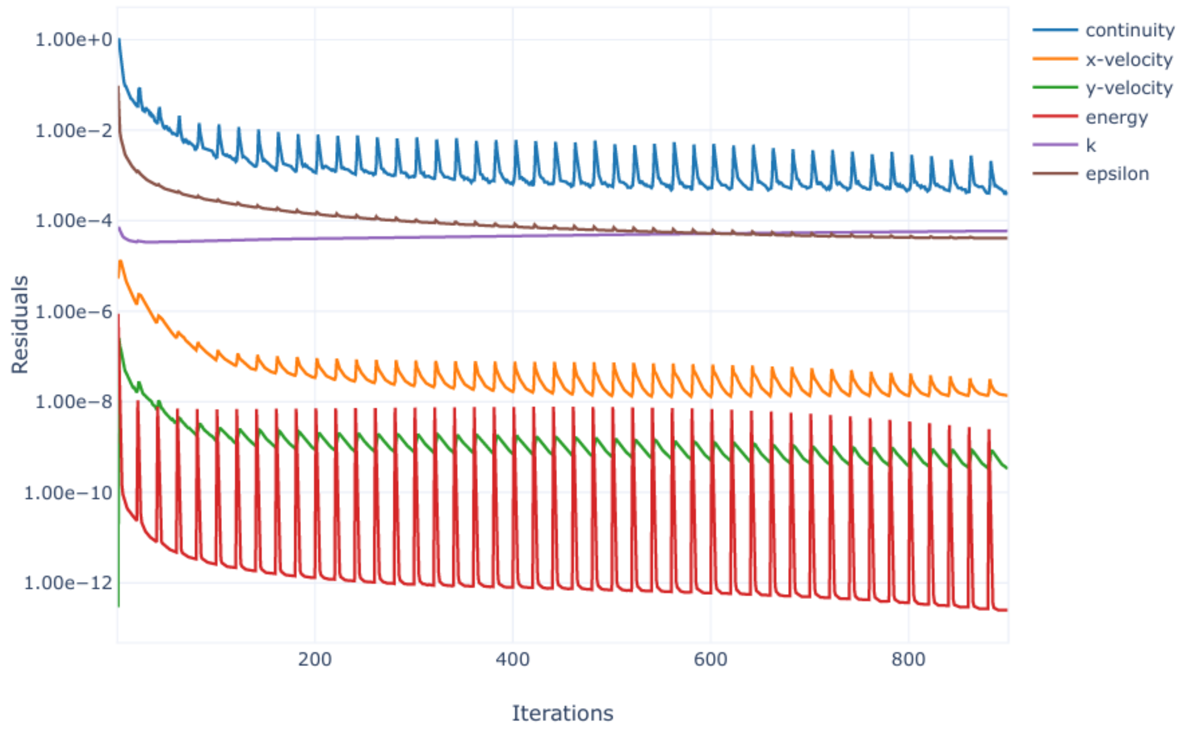

Figure 38: Residual plot from ANSYS